

A Notional Lunar Surface Rendezvous Mission In 2019

Daniel R. Adamo*

Astrodynamics Consultant, Houston, Texas 77059

In accord with currently required Ares V heavy-lift payload delivery capability to the lunar surface, a two-launch lunar surface rendezvous mission trajectory design example is presented. Notionally timed in 2019 to coincide with the fiftieth anniversary of Apollo 11's lunar landing, the first launch on June 11 delivers Earth return consumables, and the second on July 10 delivers a 4-person crew. This mission's arbitrary landing site lies near Aristarchus Crater, a destination known to pose performance difficulties to lunar exploration architectures requiring low altitude rendezvous after launch from the Moon. Performance-robbing planar trajectory corrections plaguing these architectures are demonstrated to be minimal throughout the example lunar surface rendezvous mission. In association with the nominal lunar surface rendezvous crew transport trajectory, multiple abort options are documented during the interval from trans-lunar injection until powered descent to Aristarchus landing. A crew rescue capability in deep space is also demonstrated. These viable abort and rescue scenarios further illustrate mission safety enhancements and extensibility inherent to lunar surface rendezvous.

I. Nomenclature

H	=	orbit height above reference body's equatorial radius
H _p	=	H at pericyynthion
I	=	selenocentric inertial position unit vector directed at $\delta = 0$; $\lambda = 0$
T _E	=	trans-Earth trajectory arrival epoch at geocentric $\lambda = -140^\circ$
T _L	=	effective lunar landing epoch approximately halfway between two operationally viable landing opportunities
T _M	=	trans-lunar trajectory arrival epoch at selenocentric $\lambda = -90^\circ$
T _{NLT}	=	epoch at which local morning solar elevation at the lunar landing site reaches its maximum permissible value (landing is targeted to occur no later than this time)
h	=	geodetic altitude above mean sea level
i	=	osculating orbit inclination with respect to reference body's true equatorial plane
p	=	selenocentric normal to the lunar approach trajectory plane at T _M
q	=	scalar equivalent to $ \mathbf{r}_M $
r	=	reference body-centered osculating inertial position
r _M	=	selenocentric r at epoch T _M with $\lambda = -90^\circ$
r _L	=	selenocentric inertial landing site position at epoch T _L
u	=	osculating argument of latitude with respect to reference body's true equatorial plane
v	=	reference body-centered osculating inertial velocity
v _M	=	selenocentric v at epoch T _M
Δv	=	osculating inertial velocity change magnitude
$\Delta \mathbf{v}$	=	osculating inertial velocity change vector
$\Delta \psi$	=	a time-homogeneous residual in ψ computed by subtracting a targeted trajectory's post-impulse ψ from that corresponding to an ideal or pre-impulse trajectory
δ	=	declination measured positively northward with respect to a reference body's true equatorial plane
γ	=	inertial flight path angle measured positively above the plane normal to r
λ	=	longitude measured positively eastward with respect to a reference body's prime meridian
ψ	=	inertial heading measured positively eastward with respect to a reference body's true north axial rotation projected into the plane normal to r

* Sole Proprietor, 4203 Moonlight Shadow Ct., adamod@earthlink.net, and AIAA Senior Member.

II. Introduction

Recent Constellation Program (CxP) upgrades in performance requirements imposed on the Ares V heavy-lift launch vehicle have enabled a lunar surface rendezvous (LSR) flight profile enjoying distinct advantages over currently envisioned lunar exploration architecture [1]. An LSR profile entails the following significant events.

- 1) Ares V launches a cargo-only payload into low Earth orbit (LEO). This payload consists of a return consumables module (RCM) and descent module (DM) atop the Ares V Earth departure stage (EDS). Functionally, the DM may be regarded as an *Altair* Lunar Surface Access Module (LSAM) descent stage scaled up by a mass factor of 1.17 with respect to its Exploration Systems Architecture Study (ESAS) report baseline ([2], Table 4-23, PDF p. 174).
- 2) Following a checkout period in LEO lasting at most 6 hours, EDS achieves trans-lunar injection (TLI) for the RCM/DM payload and is jettisoned.
- 3) With its RCM payload attached, the DM inserts into low lunar orbit (LLO) and lands on the Moon 3 or 4 days after launch.
- 4) Following landing, an RCM functional integrity check, including lunar landing navigation aids (navaids), is performed as a prerequisite to crew launch. These navaids serve as a precision approach and touchdown radio and/or optical beacon for subsequent landings nearby.
- 5) Up to 6 months after RCM landing and checkout, Ares V launches an *Orion* Crew Exploration Vehicle (CEV) with a crew of 4, together with a DM, into LEO atop an EDS. This CEV's Service Module (SM) has a scaled-up main engine thrust and propellant storage capacity with respect to the CEV currently being designed under Ares I launch performance constraints. The SM propellant load at Ares V launch is partial, intended only for contingency use prior to lunar landing. With respect to the ESAS report baseline ([2], Table 5-2, PDF p. 247), SM mass at Ares V launch is scaled by a factor of 0.90.
- 6) Following a checkout period in LEO lasting at most 6 hours, EDS achieves TLI for the CEV/DM payload and is jettisoned.
- 7) With its CEV payload attached, the DM inserts into LLO and lands on the Moon adjacent to the RCM 3 or 4 days after launch.
- 8) In parallel with crew lunar surface operations, SM propellant and other CEV consumables are topped off from the RCM. Following top-off, SM mass increases to a factor 2.25 times that of the previously cited ESAS baseline.
- 9) Using its DM as a launch pad, the CEV employs SM propulsion to insert into LLO and initiate return to Earth, targeting atmospheric entry within 3 to 4 days after lunar liftoff.
- 10) Shortly before Earth atmospheric entry, the CEV's SM is jettisoned, leaving the Crew Module (CM) to undergo controlled entry and landing prior to mission completion.

The foregoing LSR sequence of events is notable in at least two respects. First, crewmembers only reside in the CM cabin during outbound and return transits between Earth and the lunar surface. No other flight-worthy crew cabin with expensive life support and avionics systems need be developed. Second, crew and mission completion cargo are not brought together until the lunar surface destination is reached, eliminating orbit rendezvous and docking operations throughout the mission. By confining rendezvous to the lunar surface destination, an LSR flight profile is relieved of multiple time-dependent geometric trajectory constraints. This attribute facilitates implementing the "land anywhere; leave anytime" lunar exploration requirement imposed by United States Space Exploration Policy without incurring undesirable performance variations or timeline delays from one mission plan to another.

Current lunar exploration architecture experiences performance challenges chiefly because it requires rendezvous with a CEV in LLO after lunar landing and before Earth return by the crew can be initiated. If the landing site is at a mid-latitude lunar location, CEV may require a potentially large plane change impulse to align its LLO with this site immediately before the crew launches from it. Regardless of landing site location, another large plane change may be required following rendezvous in order to align the CEV's orbit with the lunar departure hyperbolic trajectory escape asymptote required for Earth return.

To illustrate efficient management of planar LLO constraints, this paper documents a notional LSR trajectory design targeting mid-latitude lunar landings near Aristarchus Crater. Although planetary science interest in the Aristarchus region is high, capability to reach this location with architectures requiring LLO rendezvous is marginal, particularly when the interval between crew lunar landing and launch is not optimal. The trajectory design therefore adopts a non-optimal crew landing-to-launch interval near one week. This "sortie" interval serves to demonstrate

managing $\sim 90^\circ$ of lunar rotation/revolution in geocentric space before the LSR crew returns to Earth from a mid-latitude lunar location without any significant trajectory plane change.

A secondary objective of this paper is to demonstrate CEV Earth return can be initiated at virtually any time during the LSR mission prior to nominal lunar liftoff. A propellant budget consistent with LSR vehicle capability [1, Section V] is adopted and shown to support multiple abort strategies during trans-lunar coast and from LLO prior to landing. In addition, CEV abort and rescue options assuming no LOI are demonstrated in accord with this budget.

This paper employs Coordinated Universal Time (UTC) in describing various events. In the paper's narrative, a UTC epoch is provided as a calendar date (year, month, and day of month) followed by the equivalent day-of-year (DOY), hour (hh), minute (mm), and second (ss) as precision warrants. Values relating to the latter quantities are formatted as DOY/hh:mm:ss. In trajectory plots, UTC epoch annotations appear in DOY/hh:mm format and do not contain calendar date information. All UTC epochs are associated with the year 2019, where the interval between Terrestrial Dynamical Time (TDT) and UTC, expressed as the difference TDT - UTC, is estimated to be +70 s.

The author has conducted research documented by this paper in the interest of promoting safe, robust, and cost-effective human space exploration beyond LEO. This research and its documentation were performed entirely with the author's personal time and facilities. Consequently, the broadest possible distribution of this paper without modification is encouraged free of charge to any recipient.

III. Trajectory Targeting Methods

Targeting methods applied to designing the LSR and rescue missions are summarized as follows.

- 1) Parking Orbit Mode (POM): this analytic conic targeting mode assumes instantaneous launch at a specified UTC epoch and \mathbf{r} . It then defines a circular parking orbit coasting between the launch position and a desired position offset with respect to an antipode[†] in inertial space.
- 2) Conic Solution Mode (CSM): this analytic conic targeting mode obtains a universal Lambert boundary value solution [4].
- 3) Special Perturbations Solution Mode (SPSM): this numeric integration targeting mode invokes any number of perturbations to conic motion and "shoots" at an arrival position using the WeavEncke trajectory predictor [5]. By iteratively refining a state transition matrix of arrival position partial derivatives with respect to departure velocity, SPSM computes a departure velocity yielding the specified arrival position and epoch in the presence of these perturbations [6]. Typically, SPSM is "seeded" with a departure velocity guess from a previous POM, CSM, or SPSM solution.

IV. Mission Design Ground Rules and Constraints (GR&C)

The following GR&C list is adopted for the notional LSR mission design. Each item in the list is associated with either of two possible types. An *arbitrary* GR&C is a necessary assumption or simplification to achieve the specific LSR mission design called for by this paper's demonstrative objectives, but it does not generally apply to such designs. A *mandatory* GR&C is associated with currently perceived CxP technology or infrastructure as it limits LSR architecture proposed in [1].

- 1) Arbitrary: Ares V launches occur about a month apart in 2019 such that crew lunar surface operations are in progress during the fiftieth anniversary of Apollo 11's lunar landing on July 20.
- 2) Mandatory: Ares V launches occur from the vicinity of Kennedy Space Center (KSC) Launch Complex 39 (LC-39) at true azimuths near 90° (due east).
- 3) Arbitrary: Ares V launches instantly achieve a geocentric circular orbit with $H = 185$ km, $\delta = +28.5^\circ$, and $\lambda = -80.6^\circ$.

[†] In POM, an antipode is a reference body-centered vector defined in either of two contexts within this paper's scope. The context of Earth departure for the Moon has the antipode directed opposite the Moon's geocentric position at lunar arrival. The context of lunar departure for the Earth has the antipode directed opposite selenocentric asymptotic velocity. Antipode-driven trajectory geometry is clearly illustrated by [3] in Figure 6.17 on p. 115.

- 4) Arbitrary: following Ares V launch, LSR trajectories are subject to gravitational accelerations from the Earth, Sun, and Moon at all times. When dominant among other accelerations, Earth gravitation is further perturbed by its $J_{2,0}$ Legendre (equatorial oblateness) coefficient.
- 5) Arbitrary: all propulsive translations in an LSR trajectory are instantaneous impulses. This includes powered descent to the lunar landing site from LLO.
- 6) Arbitrary: between Ares V launch and trans-lunar injection (TLI), EDS and its payload coast for an interval between one and two complete orbits.
- 7) Mandatory: to limit DM performance losses from cryogenic propellant boil-off, lunar landing occurs less than 4 days after Ares V launch.
- 8) Mandatory: to minimize Δv requirements achieving Earth return via circumlunar abort from trans-lunar flight, lunar approach will be from the Moon's western hemisphere[‡].
- 9) Arbitrary: between lunar orbit insertion and powered descent to the lunar surface, at least 12 hours are spent coasting in a circular LLO with H near 100 km to support precision tracking or crew sleep as necessary.
- 10) Mandatory: a nominal LOI impulse must not exceed $\Delta v = 910.7$ m/s, the Apollo 17 as-flown LOI reference value adopted in [1], Subsection N, to estimate DM mass in accord with Ares V performance capability.
- 11) Arbitrary: the lunar landing site near Aristarchus Crater is located at selenocentric $\delta = +26^\circ$ and $\lambda = -49^\circ$ and is named Aristarchus Plateau ([7], p. 20).
- 12) Arbitrary: lunar landings occur with local morning solar elevation between $+5^\circ$ and $+15^\circ$.
- 13) Arbitrary: the nominal/primary lunar landing orbit is the first (easterly) of two consecutive orbits whose ground tracks bracket the landing site. The second (westerly) of these orbits is a backup/secondary landing opportunity compliant with all applicable GR&C items.
- 14) Arbitrary: the interval between nominal crew lunar landing and launch is between 7 and 8 days.
- 15) Arbitrary: crew lunar launch instantly achieves a selenocentric circular orbit with $H = 100$ km, $\delta = +26^\circ$, and $\lambda = -49^\circ$.
- 16) Arbitrary: from lunar launch to trans-Earth injection (TEI), CEV coasts for an interval between one and two complete orbits.
- 17) Mandatory: a nominal TEI impulse must not exceed $\Delta v = 928.5$ m/s, the Apollo 17 as-flown TEI reference value adopted in [1], Subsection O, to estimate SM mass in accord with Ares V performance capability.
- 18) Arbitrary: the interval from nominal TEI to Earth atmospheric entry interface (EI) is 3 to 4 days.
- 19) Mandatory: EI is at $h = 121.92$ km and $\gamma = -5.86^\circ \pm 0.5^\circ$ with ψ eastbound.
- 20) Arbitrary: upon return from the Moon, targeted CEV Earth arrival is at epoch T_E and geocentric $\lambda = -140^\circ \pm 0.5^\circ$ with ψ northbound and $i = 30^\circ \pm 5^\circ$. Note EI will generally be at a slightly different longitude.
- 21) Mandatory: post-TLI, the crew must not expend more than $\Delta v = 3015$ m/s (as documented in [1], Subsection N) from the DM in arriving at and recovering from an abort, assuming DM propulsion still functions.
- 22) Mandatory: following DM jettison, the crew must not expend more than $\Delta v = 907$ m/s (as documented in [1], Subsection O) from the SM in recovering from an abort, assuming SM propulsion still functions.

Specific items in the foregoing list will subsequently be cited in this paper as "GR&C #N", with N corresponding to the listed item's enumeration.

V. Outbound RCM/DM Transit

In accord with GR&C #1's mission scheduling, the time at which the local morning Sun reaches an elevation of $+15^\circ$ at the GR&C #11 Aristarchus Plateau landing site is determined using the Jet Propulsion Laboratory's (JPL's) *Horizons* telnet server [8] to be 2019 June 15 at 166/18:54 UTC. This T_{NLT} epoch becomes a "no later than" RCM/DM landing time under GR&C #12 solar elevation limits.

[‡] According to selenocentric convention adopted by this paper, the Moon's western hemisphere is its leading hemisphere with respect to motion in its geocentric orbit.

To honor maximum outbound transit time under GR&C #7 and #9, a preliminary interval of 3 days is allotted to transit from TLI to LOI. The June 11 launch time conforming to this interval, GR&C #2 and #3 launch geometry, and GR&C #6 transit time from launch to TLI is then sought using POM targeting. The POM solution subsequently seeds SPSM targeting of launch and antipode Earth parking orbit positions in accord with GR&C #4 acceleration modeling. Expressed in Earth mean equator and equinox of epoch J2000.0 (J2K) coordinates under GR&C #3's instantaneous launch ground rule, the SPSM solution is equivalent to the following state vector.

State #1: RCM/DM instantaneous KSC launch on 2019 June 11 at 162/19:39 UTC

$$\mathbf{r} = \begin{bmatrix} -2317.846 \\ +5278.957 \\ +3136.074 \end{bmatrix} \text{ geocentric J2K km} \quad \mathbf{v} = \begin{bmatrix} -7.125761 \\ -3.161770 \\ +0.057118 \end{bmatrix} \text{ geocentric J2K km/s}$$

$$i = 28.502^\circ \quad u = 89.328^\circ \quad \psi = 89.635^\circ \quad \gamma = +0.005^\circ$$

A byproduct of the launch-to-TLI POM solution is a preliminary TLI epoch. Geocentric position associated with State #1 coasted to this epoch with GR&C #4 acceleration modeling becomes the departure boundary condition for CSM iterations determining the preliminary RCM/DM geocentric trans-lunar ellipse. Because "short-way" CSM solutions are sought with geocentric transfer angles less than 180° , iterations required to obtain a satisfactory CSM solution consist of adjustments to the POM solution's TLI epoch. These adjustments drive TLI late enough to ensure the transfer ellipse is posigrade, yet not so late that departure γ becomes positive by more than a fraction of a degree.

Selenocentric arrival boundary conditions associated with any trans-lunar trajectory in this mission design warrant elaboration. To satisfy GR&C #7's maximum transit time from launch to landing at Aristarchus Plateau, while not exceeding GR&C #10's maximum LOI Δv , trans-lunar arrival at epoch T_M is ideally in a selenocentric trajectory plane containing \mathbf{r}_L , the landing site's inertial location at the effective landing epoch T_L §. With \mathbf{r}_L known, the required trans-lunar selenocentric approach trajectory plane is defined by selenocentric arrival velocity \mathbf{v}_M .

In a manner akin to B-plane targeting ([3], Figure 6.18, p. 117)** , the explicit trans-lunar arrival boundary condition \mathbf{r}_M is computed as follows.

$$\mathbf{p} = \pm(\mathbf{v}_M \times \mathbf{r}_L) \tag{1}$$

$$\mathbf{r}_M = q \frac{\mathbf{p} \times \mathbf{I}}{|\mathbf{p} \times \mathbf{I}|} \tag{2}$$

The sign ambiguity in Equation 1 is easily resolved because lunar approach must be from the Moon's western hemisphere under GR&C #8. This constraint effectively requires retrograde selenocentric motion with \mathbf{p} pointed into the Moon's southern hemisphere. Equation 2's scalar q is iterated to achieve $H_p = +100$ km, fulfilling GR&C #9's targeted LLO H. Selenocentric geometry associated with Equations 1 and 2 is illustrated in Figure 1. Note the gray-shaded \mathbf{r}_L , \mathbf{v}_M , and \mathbf{p} vectors are, in general, projections into the targeting plane along with approach trajectory points. The unit vector \mathbf{I} is normal to the target plane and directed at the Figure 1 viewer.

§This ideal geometry must be compromised slightly such that two successive lunar ground tracks straddle Aristarchus Plateau to the east and west in accord with GR&C #13. With LLO period post-LOI very near 2 hours, LOI located above the Moon's farside, and Aristarchus Plateau located on the Moon's nearside, a satisfactory straddle can be achieved by requiring $T_L - T_M$ to be an even number of hrs.

** As stated in [3], the B-plane is orthogonal to a hyperbolic trajectory's approach asymptote and displaced "a large distance from" the reference body. Neither condition is honored by the technique documented here. As evident from Figure 1, the plane in which LSR lunar approaches are targeted nearly coincides with the Moon's Earth-facing hemisphere and contains the Moon's center.

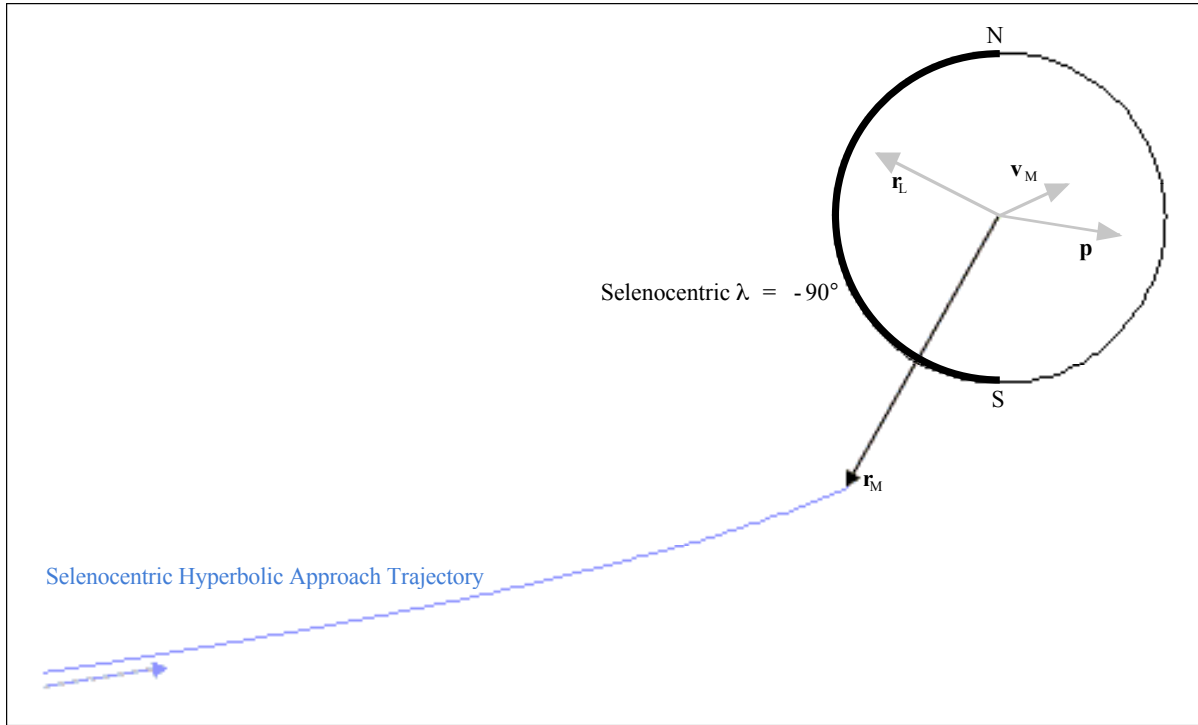


Figure 1: The Selenocentric Lunar Approach Targeting Plane Containing r_M

In practice, an initial guess at r_M (selenocentric $H = 1000$ km, $\delta = 0$, $\lambda = -90^\circ$ can be used in lieu of better information) is sufficient to obtain a CSM trans-lunar trajectory serving as preliminary seed to successive SPSM iterations with GR&C #4 acceleration modeling. Each SPSM trans-lunar solution provides a v_M with which to refine r_M . The primary goal in performing multiple SPSM iterations is to achieve a post-TLI ψ matching that of the pre-TLI Earth parking orbit. To achieve a ψ match, T_M is modified as required. During this process, it will generally be necessary to adjust q on occasion to maintain H_p near +100 km.

When trans-lunar SPSM iterations are complete for the RCM/DM trajectory, r_M and T_M have converged to selenocentric $H = +1499.8$ km, $\delta = -60.5^\circ$, and $\lambda = -90^\circ$ on June 15 at 166/02:56 UTC, assuming $T_L - T_M = +14$ hrs. The converged SPSM trans-lunar solution, expressed as a post-TLI state vector under GR&C #5's impulsive translation ground rule, is as follows.

State #2: RCM/DM post-TLI on 2019 June 11 at 162/22:24 UTC (TLI $\Delta v = 3147.214$ m/s)

$$\mathbf{r} = \begin{bmatrix} +2730.312 \\ +5560.291 \\ +2168.497 \end{bmatrix} \text{ geocentric J2K km} \quad \mathbf{v} = \begin{bmatrix} -9.660838 \\ +3.419064 \\ +3.835466 \end{bmatrix} \text{ geocentric J2K km/s}$$

$$i = 28.547^\circ \quad u = 43.868^\circ \quad \psi = 68.585^\circ \quad \gamma = +0.759^\circ$$

When the trans-lunar RCM/DM trajectory reaches pericyynthion, an impulsive LOI translation compliant with GR&C #5 and #9 produces the following LLO state vector. Note retrograde LOI Δv easily satisfies the maximum permissible value of 910.7 m/s imposed by GR&C #10.

State #3: RCM/DM post-LOI on 2019 June 15 at 166/03:20:40.360 UTC (LOI $\Delta v = 862.304$ m/s)

$$\mathbf{r} = \begin{bmatrix} -1445.964 \\ +96.408 \\ -1130.699 \end{bmatrix} \text{ selenocentric J2K km} \quad \mathbf{v} = \begin{bmatrix} -1.008259 \\ -0.092209 \\ +1.281499 \end{bmatrix} \text{ selenocentric J2K km/s}$$

$$i = 109.498^\circ \quad u = 323.295^\circ \quad \psi = 336.171^\circ \quad \gamma = +0.001^\circ$$

Shortly after LOI, RCM/DM passes its first ascending node on the lunar equator, beginning LLO #1 under this mission design's counting convention. State #3 is coasted under GR&C #4 acceleration modeling to verify GR&C #13 is satisfied with successive ground tracks immediately east and west of Aristarchus Plateau, bracketing the targeted $T_L = T_M + 14$ hrs (June 15 at 166/16:56 UTC). As RCM/DM proceeds on a southwesterly path above the

Moon's Ocean of Storms on LLO #7, GR&C #5 infers an instantaneous Aristarchus Plateau landing from the east on June 15 at 166/16:09 UTC with +13.8° local morning solar elevation. On LLO #8, instantaneous landing from the west is at 166/18:07 UTC with +14.6° morning solar elevation. Under GR&C #13, the LLO #7 landing is considered primary, and the LLO #8 landing is secondary. Both landings satisfy GR&C #7's landing deadline (4 days after launch, or no later than June 15 at 166/19:39 UTC), GR&C #9 minimum time from LOI to landing, and morning solar elevation limits at landing imposed by GR&C #12.

VI. Outbound CEV/DM Transit

In accord with GR&C #1's mission scheduling, the time at which the local morning Sun reaches an elevation of +15° at the GR&C #11 Aristarchus Plateau landing site is determined using JPL *Horizons* [8] to be 2019 July 15 at 196/05:00 UTC. This epoch is the latest permissible CEV/DM landing time under GR&C #12 solar elevation limits.

To honor maximum outbound transit time under GR&C #7 and #9, a preliminary interval of 3 days is allotted to transit from TLI to LOI. The July 10 launch time conforming to this interval, GR&C #2 and #3 launch geometry, and GR&C #6 transit time from launch to TLI is then sought using POM targeting. The POM solution subsequently seeds SPSM targeting of launch and antipode Earth parking orbit positions in accord with GR&C #4 acceleration modeling. Expressed as an instantaneous launch state vector, the SPSM solution is as follows.

State #4: CEV/DM instantaneous KSC launch on 2019 July 10 at 191/18:22 UTC

$$\mathbf{r} = \begin{bmatrix} -3138.699 \\ +4835.154 \\ +3137.612 \end{bmatrix} \text{ geocentric J2K km} \quad \mathbf{v} = \begin{bmatrix} -6.519128 \\ -4.274666 \\ +0.067202 \end{bmatrix} \text{ geocentric J2K km/s}$$

$$i = 28.503^\circ \quad u = 89.155^\circ \quad \psi = 89.541^\circ \quad \gamma = +0.004^\circ$$

A byproduct of the launch-to-TLI POM solution is a preliminary TLI epoch. Geocentric position associated with State #4 coasted to this epoch with GR&C #4 acceleration modeling becomes the departure boundary condition for CSM iterations determining the preliminary CEV/DM geocentric trans-lunar ellipse. Because "short-way" CSM solutions are sought with geocentric transfer angles less than 180°, iterations required to obtain a satisfactory CSM solution consist of adjustments to the POM solution's TLI epoch. These adjustments drive TLI late enough to ensure the transfer ellipse is posigrade, yet no so late that departure γ becomes positive by more than a fraction of a degree.

An initial guess at \mathbf{r}_M (selenocentric $H = 1000$ km, $\delta = 0$, $\lambda = -90^\circ$ can be used in lieu of better information) is sufficient to obtain a CSM trans-lunar solution serving as preliminary seed to successive SPSM iterations with GR&C #4 acceleration modeling. Each SPSM trans-lunar solution provides a \mathbf{v}_M with which to refine \mathbf{r}_M . The primary goal in performing multiple SPSM iterations is to achieve a post-TLI ψ matching that of the pre-TLI Earth parking orbit. To achieve a ψ match, T_M is modified as required. During this process, it will generally be necessary to adjust q on occasion to maintain H_p near +100 km.

When trans-lunar SPSM iterations are complete for the CEV/DM trajectory, \mathbf{r}_M and T_M have converged to selenocentric $H = +1027.7$ km, $\delta = -71.5^\circ$, $\lambda = -90^\circ$ on July 13 at 194/23:50 UTC, assuming $T_L - T_M = 16$ hrs. The converged SPSM trans-lunar solution, expressed as a post-TLI state vector under GR&C #5's impulsive translation ground rule, is as follows.

State #5: CEV/DM post-TLI on 2019 July 10 at 191/21:10 UTC (TLI $\Delta v = 3151.525$ m/s)

$$\mathbf{r} = \begin{bmatrix} +465.855 \\ +6009.313 \\ +2597.131 \end{bmatrix} \text{ geocentric J2K km} \quad \mathbf{v} = \begin{bmatrix} -10.533580 \\ -0.412394 \\ +2.955554 \end{bmatrix} \text{ geocentric J2K km/s}$$

$$i = 28.504^\circ \quad u = 56.043^\circ \quad \psi = 73.126^\circ \quad \gamma = +0.232^\circ$$

Centered on the CEV/DM's mid-Atlantic location 1 hour 45 minutes after Ares V launch (as displayed in the "mission elapsed time", or "MET", window), the Figure 2 ground track plot illustrates how the Earth parking orbit is altered following TLI north of Hawaii at 2 hours 48 minutes MET. As the post-TLI ground track moves over northern Brazil, CEV/DM geocentric eastward inertial angular rate becomes less than that of locations rotating with Earth's surface beneath the spacecraft, causing the ground track to begin a westward drift towards Peru and the Pacific Ocean. Meanwhile, CEV/DM orbit height increases from 185 km in the parking orbit to 58000 km over central Peru. Individual ground track points, discernable in the parking orbit, are plotted at 30-second intervals. The region of Earth's surface appearing with a black background is in darkness at 1 hour 45 minutes MET (20:07 UTC), with the Sun about to set on London, England. Relative to this "current" time, the "Sun" window indicates CEV will undergo a sunset in 5 minutes 29 seconds.

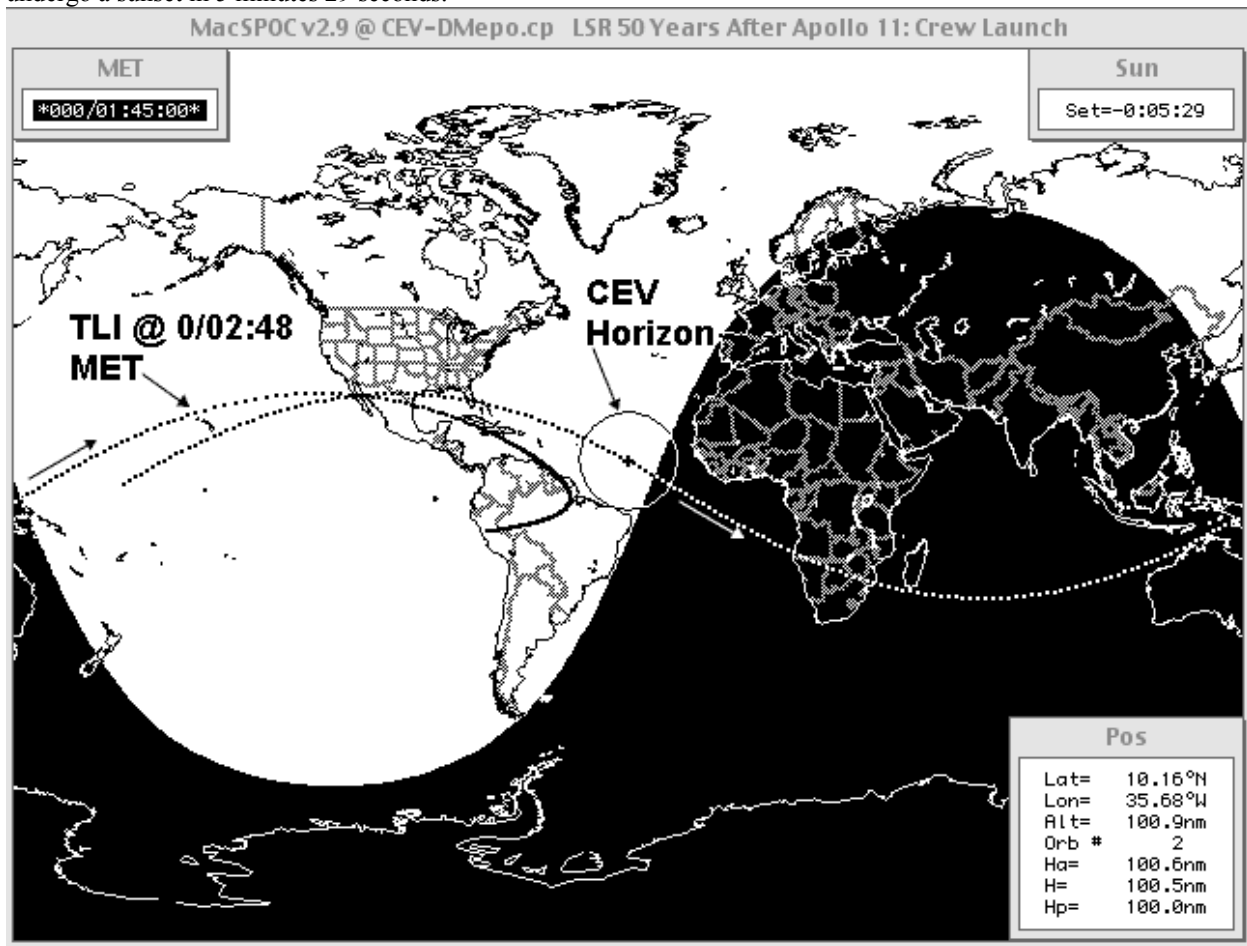


Figure 2: CEV/DM Earth Departure Ground Track

When the trans-lunar CEV/DM trajectory reaches pericyynthion, an impulsive LOI translation compliant with GR&C #5 and #9 produces the following LLO state vector. Note retrograde LOI Δv easily satisfies the maximum permissible value of 910.7 m/s imposed by GR&C #10.

State #6: CEV/DM post-LOI on 2019 July 14 at 195/00:08:39.850 UTC (LOI $\Delta v = 874.668$ m/s)

$$\mathbf{r} = \begin{bmatrix} -1174.842 \\ -312.378 \\ -1377.805 \end{bmatrix} \text{ selenocentric J2K km} \quad \mathbf{v} = \begin{bmatrix} -1.065236 \\ -0.648069 \\ +1.055253 \end{bmatrix} \text{ selenocentric J2K km/s}$$

$i = 102.925^\circ$ $u = 321.983^\circ$ $\psi = 343.759^\circ$ $\gamma = +0.000^\circ$

Time ticks ("+" icons) in the Figure 3 plot are annotated in UTC DOY/hh:mm format, where DOY = 192 to 195 = July 11 to 14. Dotted lines emanating from time ticks are projections onto the ecliptic plane. The LOI event is not labeled to avoid excessive clutter, but its effects are evident as the trans-lunar trajectory is transformed into a tight helix about the Moon's geocentric orbit. Earth's nighttime hemisphere is shaded.

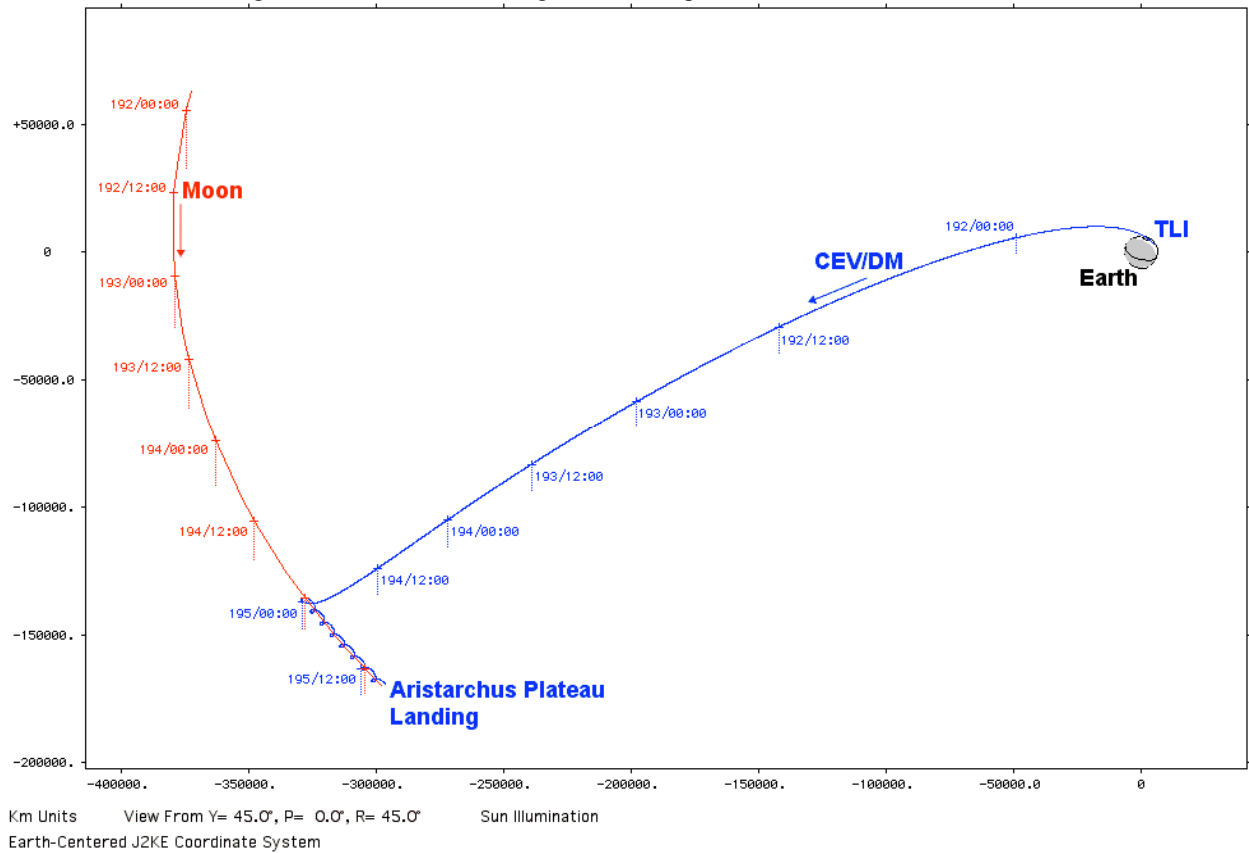
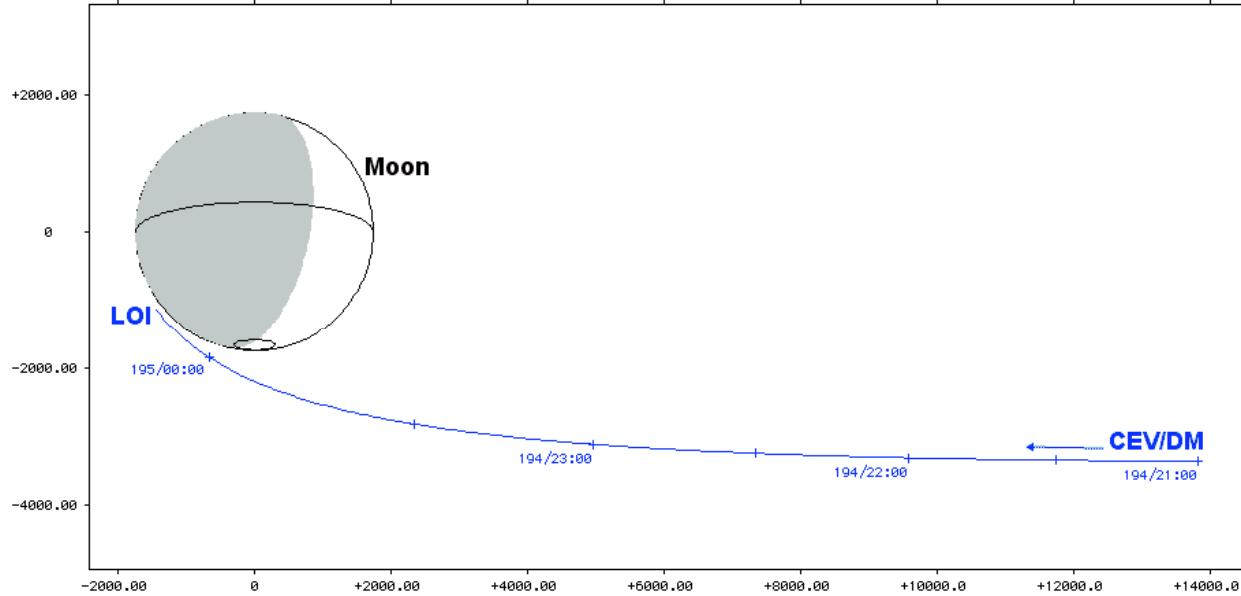


Figure 3: CEV/DM Outbound Transit From TLI To Lunar Landing

The final several hours of trans-lunar CEV/DM flight are plotted relative to the Moon in Figure 4, ending with lunar orbit insertion (LOI) 100 km above the Moon's surface shortly after UTC DOY = 195 = July 14 begins. Shaded points of the Moon's surface are located on its farside from Earth. The plot's plane very nearly coincides with that of CEV/DM's selenocentric approach hyperbolic trajectory and post-LOI circular lunar orbit. During the 15 hours from LOI to lunar landing, the Aristarchus Plateau landing site will shift location slightly eastward as the Moon rotates with respect to the plot plane. When landing occurs, Aristarchus Plateau will be very near the plot plane at a lunar limb position close to Figure 4's "Moon" annotation.



Km Units View From Y=335.0°, P= 0.0°, R=104.5° Earth Illumination
Moon-Centered EPM Coordinate System @ 2019y 195d (7-14) 0: 0 UTC

Figure 4: CEV/DM Lunar Arrival

Shortly after LOI, CEV/DM passes its first ascending node on the lunar equator, beginning LLO #1 under this mission design's counting convention. State #6 is coasted under GR&C #4 acceleration modeling to verify GR&C #13 is satisfied with successive ground tracks immediately east and west of Aristarchus Plateau, bracketing the targeted $T_L = T_M + 16$ hrs (July 14 at 195/15:50 UTC). As CEV/DM proceeds on a southwesterly path above the Moon's Ocean of Storms on LLO #8, GR&C #5 infers an instantaneous Aristarchus Plateau landing from the east on July 14 at 195/14:56 UTC with +8.6° local morning solar elevation. On LLO #9, instantaneous landing from the west is at 16:54 UTC with +9.5° local morning solar elevation. Under GR&C #13, the LLO #8 landing is considered primary, and the LLO #9 landing is secondary. Both landings satisfy GR&C #7's landing deadline (4 days after launch, or no later than July 14 at 195/18:22 UTC), GR&C #9 minimum time from LOI to landing, and morning solar elevation limits at landing imposed by GR&C #12.

Approach ground tracks to Aristarchus Plateau (blue dot) on CEV/DM LLO #8 (green ground track) and LLO #9 (red ground track) are plotted in Figure 5. Time ticks at 30-second intervals on each ground track are annotated with July 14 UTC in hh:mm:ss format. The lunar map in Figure 5's background is a segment of *Aristarchus LAC 39* [9].

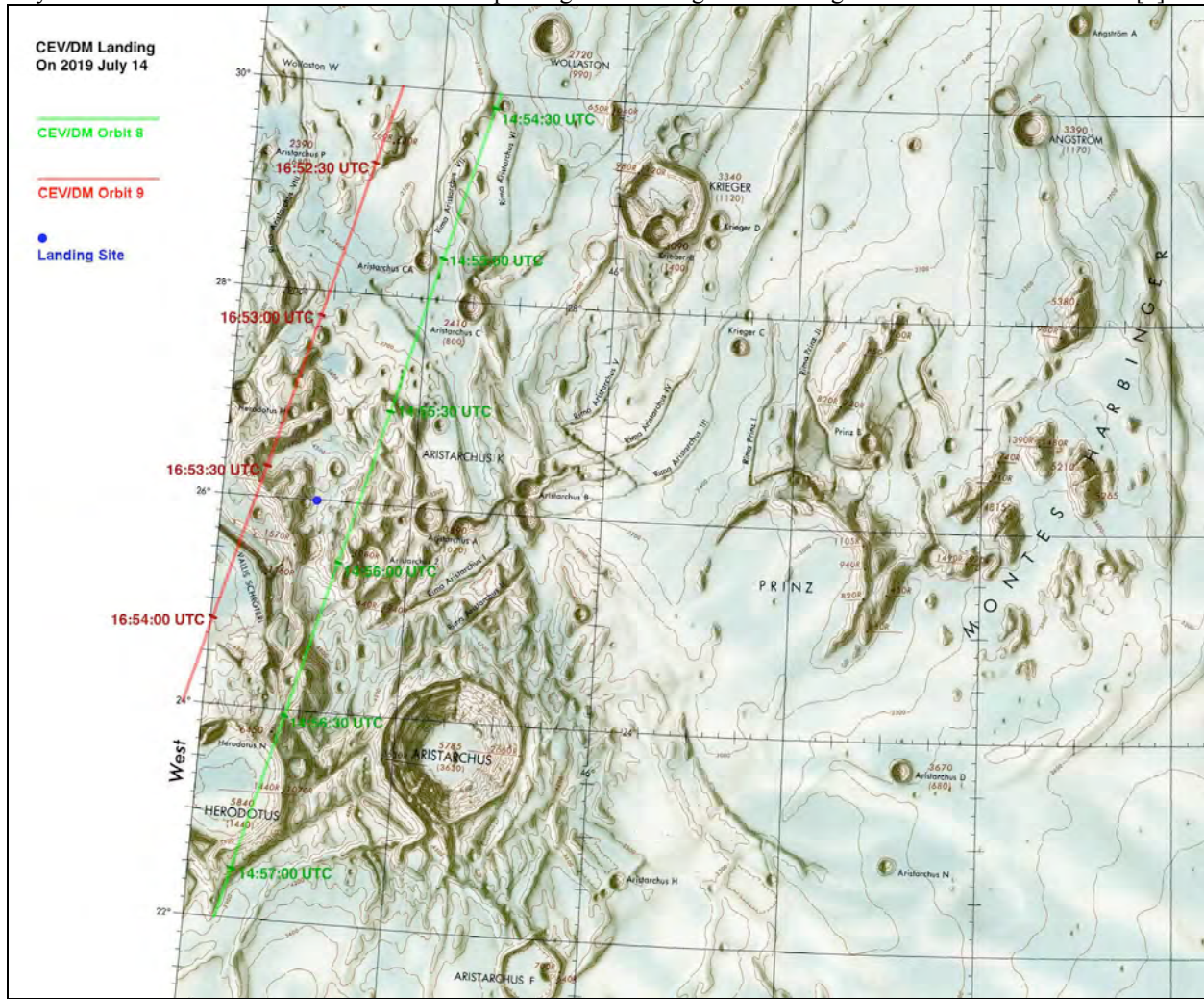


Figure 5: 2019 July 14 CEV/DM Aristarchus Plateau Approach Ground Tracks

VII. Return CEV Transit

Because LSR architecture requires no LLO rendezvous during Earth return, launch ψ from Aristarchus Plateau is unconstrained by that LLO plane's orientation. In addition, the Moon's inertial rotation rate is so slow (equivalent to 4.2 m/s selenocentric eastward velocity at Aristarchus Plateau) that ψ -dependent launch performance penalties are insignificant at any lunar surface location. Consequently, launch and TEI can be targeted in the context of an intermediate westbound (retrograde) or eastbound (posigrade) LLO. Since posigrade selenocentric trajectories were never flown during the Apollo Program, the following subsections present Earth return solutions from analogous retrograde and posigrade LLO.

In compliance with GR&C #1, CEV launch from Aristarchus Plateau, cannot occur before the fiftieth anniversary of Apollo 11's *Tranquility Base* landing on July 20 at 201/20:17:39 UTC ([10], p. 322). Moreover, GR&C #14 requires launch be in the interval from 7 to 8 days after CEV/DM landing (equivalent to a one-day launch window opening on July 21 at 202/14:56 UTC). The interval from GR&C #15's instantaneous Aristarchus Plateau launch into LLO is between 1 and 2 complete orbits (a time interval between 2 and 4 hrs at GR&C #15 $H = 100$ km), placing the earliest possible TEI on July 21 at 202/16:56 UTC.

Selenocentric lunar departure trajectories following trans-Earth injection (TEI), resulting from both LLO options, are plotted in Figure 6 as UTC DOY = 202 = July 21 draws to a close. The plot plane very nearly coincides with the Aristarchus Plateau launch site, both LLO planes (omitted to avoid excessive clutter), and both lunar departure hyperbolic trajectories. Dotted lines emanating from time ticks are projections onto the lunar equatorial plane. Shaded points on the Moon's surface are located on its farside from Earth.

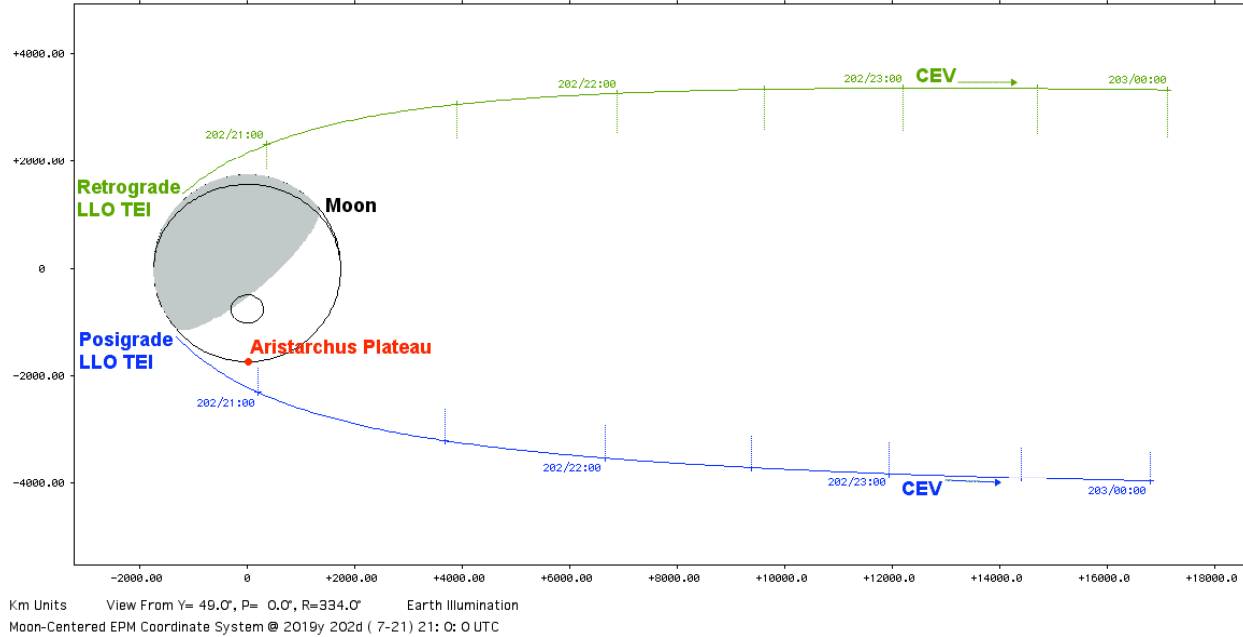


Figure 6: Two CEV Lunar Departure Options

A. Retrograde LLO Prior To CEV Lunar Departure

To initiate determination of a T_E epoch leading to satisfactory EI conditions under GR&C #19 and #20, CSM targeting is invoked with TEI departure notionally specified on July 21 at 202/20:48 UTC (about 4 hrs after the earliest possible TEI) and T_E about 75 hrs later^{††}. Fixed CSM boundary conditions are lunar departure $H = 100$ km, $\delta = 0$, and $\lambda = 180^\circ$ along with Earth arrival $H = 121.92$ km^{‡‡} and $\lambda = -140^\circ$. As arrival epoch is varied to obtain geocentric trans-Earth short-way CSM solutions, arrival γ near -5.86° is sought under GR&C #19 at a particular arrival δ . During UTC departure epochs of interest late on July 21, the Moon's geocentric δ is near -7° , placing the Moon's geocentric antipode δ near $+7^\circ$. With northbound arrival ψ to be obtained in accord with GR&C #20, arrival δ somewhat south of $+7^\circ$ is therefore required because $EI < 0$ is sought. After arrival epochs T_E yielding γ near -5.86° are determined for two δ values bracketing $i = 30^\circ$, a δ can be linearly interpolated at which the desired ψ will be obtained at the T_E having γ near the desired -5.86° . From the CSM solution thus iterated, EI arrival is July 24 at 205/23:46 UTC with $\delta = -2.8^\circ$ and $i = 30.172^\circ$. This " T_E/δ iteration" is utilized repeatedly by nominal and abort trans-Earth trajectory designs documented by this paper. Table 1 presents T_E/δ iteration data for this CSM solution.

^{††} Although GR&C #18 permits TEI-to-EI transits as short as 72 hrs, at least some 72-hr transit trajectory solutions for July 21 lunar departure violate GR&C #17's maximum permissible TEI Δv . If transit time is increased to 75 hrs, these violations are averted.

^{‡‡} This H boundary value must be considered preliminary in the context of GR&C #19 because EI occurs at an Earth δ -dependent *geodetic altitude* h ; not a *height* H with respect to a sphere having Earth's equatorial radius.

Table 1: CSM T_E/δ Iterations Leading To A Short-Way Trans-Earth Solution From Retrograde LLO

T_E (July 24 UTC)	Arrival δ	Arrival ψ	Arrival γ	Arrival i
205/23:00	0.0°	75.606°	-10.483°	14.394°
205/23:40		68.880°	-5.771°	21.120°
205/24:00		62.276°	-3.533°	27.724°
205/23:00	-5.0°	67.413°	-11.283°	23.106°
205/23:51		52.795°	-5.808°	37.491°
205/24:00		48.430°	-4.959°	41.815°
205/23:00	-2.8°	70.904°	-10.889°	19.293°
205/23:46		59.946°	-5.710°	30.172°
205/24:00		53.924°	-4.272°	36.170°

When an acceptable CSM trans-Earth solution is obtained, the corresponding selenocentric departure velocity is adopted as preliminary lunar escape asymptotic velocity and input to selenocentric POM targeting. Under GR&C #16, LLO coast is limited by POM to an interval between 1 and 2 orbits, while launch epoch is iterated until the POM arrival epoch matches that of the seeding CSM solution's departure epoch, July 21 at 202/20:48 UTC. State #7 is the retrograde LLO POM departure solution.

State #7: CEV instantaneous Aristarchus Plateau launch on 2019 July 21 at 202/18:07:04 UTC

$$\mathbf{r} = \begin{bmatrix} -969.538 \\ +920.274 \\ +1260.796 \end{bmatrix} \text{ selenocentric J2K km} \quad \mathbf{v} = \begin{bmatrix} +1.319723 \\ +0.890790 \\ +0.364651 \end{bmatrix} \text{ selenocentric J2K km/s}$$

$$i = 153.895^\circ \quad u = 94.950^\circ \quad \psi = 267.579^\circ \quad \gamma = +0.000^\circ$$

At this point, GR&C #4 acceleration modeling is introduced. State #7 is first coasted to the POM arrival epoch. Terminal position from this coast and pericyynthion escape velocity from the POM solution together seed an initial SPSM trans-Earth trajectory solution. Arrival boundary conditions for SPSM are inherited from the iterated CSM trans-Earth solution. In practice, only minor alterations to the initial SPSM trans-Earth solution are necessary. Sub-minute adjustments to the departure epoch drive departure γ to a small positive value, and changes to arrival H are necessary to compensate for Earth oblateness at the desired arrival $\delta = -2.8^\circ$. State #8 is the SPSM trans-Earth solution immediately after TEI from the retrograde LLO.

State #8: CEV post-TEI on 2019 July 21 at 202/20:47:40 UTC (TEI $\Delta v = 924.989$ m/s)

$$\mathbf{r} = \begin{bmatrix} +1757.414 \\ +157.670 \\ -512.913 \end{bmatrix} \text{ selenocentric J2K km} \quad \mathbf{v} = \begin{bmatrix} -0.300843 \\ -1.876968 \\ -1.711931 \end{bmatrix} \text{ selenocentric J2K km/s}$$

$$i = 153.855^\circ \quad u = 225.647^\circ \quad \psi = 251.060^\circ \quad \gamma = +0.651^\circ$$

State #9 is State #8 coasted to EI.

State #9: CEV EI on 2019 July 24 at 205/23:44 UTC (geocentric speed = 11.014 km/s)

$$\mathbf{r} = \begin{bmatrix} -6026.715 \\ +2415.576 \\ -306.210 \end{bmatrix} \text{ geocentric J2K km} \quad \mathbf{v} = \begin{bmatrix} -2.627616 \\ -8.797400 \\ +6.083090 \end{bmatrix} \text{ geocentric J2K km/s}$$

$$i = 33.500^\circ \quad u = 354.922^\circ \quad \psi = 56.604^\circ \quad \gamma = -5.835^\circ$$

B. Posigrade LLO Prior To CEV Lunar Departure

Lunar departure from a posigrade LLO is targeted in a manner nearly identical to the retrograde LLO solution documented in the previous subsection. During trans-Earth CSM targeting with T_E/δ iterations, the only fixed boundary condition difference is lunar departure $\lambda = -90^\circ$ (vice $\lambda = 180^\circ$ applied to the retrograde LLO case). From the iterated CSM solution, T_E is July 24 at 205/23:47 UTC, $\delta = -2.9^\circ$, and $i = 30.244^\circ$.

State #10 is the posigrade LLO POM solution adopting the CSM solution's selenocentric departure velocity as its asymptotic lunar escape velocity.

State #10: CEV instantaneous Aristarchus Plateau launch on 2019 July 21 at 202/17:03:48 UTC

$$\mathbf{r} = \begin{bmatrix} -955.835 \\ +928.836 \\ +1264.974 \end{bmatrix} \text{ selenocentric J2K km} \quad \mathbf{v} = \begin{bmatrix} -1.326408 \\ -0.886085 \\ -0.351627 \end{bmatrix} \text{ selenocentric J2K km/s}$$

$$i = 26.142^\circ \quad u = 84.243^\circ \quad \psi = 87.181^\circ \quad \gamma = +0.000^\circ$$

With the exception of specific boundary values, SPSM trans-Earth targeting for a posigrade LLO lunar departure is procedurally identical to the retrograde LLO departure option previously documented. State #11 is the SPSM trans-Earth solution immediately after TEI from a posigrade LLO.

State #11: CEV post-TEI on 2019 July 21 at 202/20:48 UTC (TEI $\Delta v = 916.729$ m/s)

$$\mathbf{r} = \begin{bmatrix} +68.706 \\ +1331.879 \\ +1264.075 \end{bmatrix} \text{ selenocentric J2K km} \quad \mathbf{v} = \begin{bmatrix} -2.457342 \\ -0.392480 \\ +0.557405 \end{bmatrix} \text{ selenocentric J2K km/s}$$

$$i = 26.130^\circ \quad u = 49.409^\circ \quad \psi = 72.298^\circ \quad \gamma = +0.159^\circ$$

State #12 is State #11 coasted to EI.

State #12: CEV EI on 2019 July 24 at 205/23:47 UTC (geocentric speed = 11.010 km/s)

$$\mathbf{r} = \begin{bmatrix} -6057.361 \\ +2336.281 \\ -317.537 \end{bmatrix} \text{ geocentric J2K km} \quad \mathbf{v} = \begin{bmatrix} -2.567654 \\ -8.907924 \\ +5.939417 \end{bmatrix} \text{ geocentric J2K km/s}$$

$$i = 32.618^\circ \quad u = 354.614^\circ \quad \psi = 57.497^\circ \quad \gamma = -5.729^\circ$$

The geometry between TEI Δv and the CEV-to-Earth line-of-sight is remarkable in the case of lunar departure from a posigrade LLO. From CEV, these two vectors subtend an angle of only 14° . Moreover, as is evident from Figure 6, Earth is visible from CEV during posigrade LLO lunar departure TEI, whereas Earth is behind the Moon from CEV during retrograde LLO lunar departure TEI. In the posigrade LLO lunar departure TEI case, consider a yaw/pitch Euler sequence from pre-TEI selenocentric velocity projected into the local horizontal plane with the CEV starting in neutral "heads up; +roll axis forward" attitude. A yaw/pitch of $+0.1^\circ/+0.4^\circ$ aligns the CEV +roll axis with TEI Δv , and a yaw/pitch of $+13.2^\circ/+5.6^\circ$ aligns the CEV +roll axis with the geocenter.

With the posigrade LLO lunar departure option offering Earth as an attitude reference and direct source of ground support communications during and after TEI, it is chosen over the retrograde LLO option for the notional Aristarchus Plateau mission profile developed by this paper. In another LSR mission design case, where terrain avoidance is considered in selecting lunar launch ψ , retrograde lunar departure may be the preferred option.

Geocentric Earth return following posigrade LLO lunar departure is plotted in Figure 7. Time ticks in this plot are annotated with UTC DOY = 203 to 205 = July 22 to 24. Dotted lines emanating from time ticks are projections onto the ecliptic plane. The shaded region of Earth's surface is in darkness.

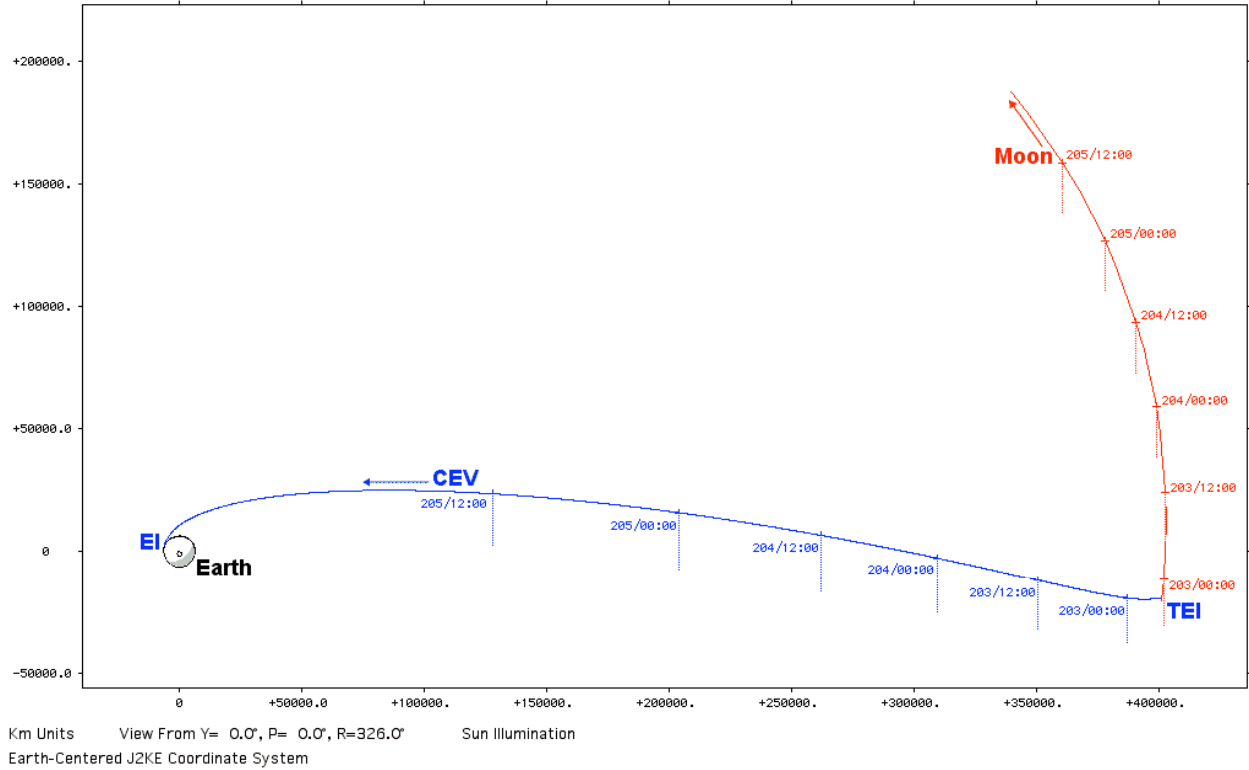


Figure 7: CEV Earth Return From TEI to EI

Starting from a location nearly 51400 km above central Australia 14 days 2 hours after launch, the Figure 8 ground track plot illustrates CEV's return to Earth, with EI less than 3.5 hours later at an altitude of 121.92 km. Individual ground track points, discernable in the vicinity of EI, are plotted at 30-second intervals. The region of Earth's surface appearing with a black background is in darkness at 14 days 2 hours MET (July 24 at 205/20:22 UTC). This surface shading, together with the "Sun" window, indicate the CEV will be in sunlight throughout the remainder of its return to Earth. Depending on entry systems ultimately developed for CEV lunar missions, this EI could lead to splashdown in the eastern Pacific Ocean or landing in North America.

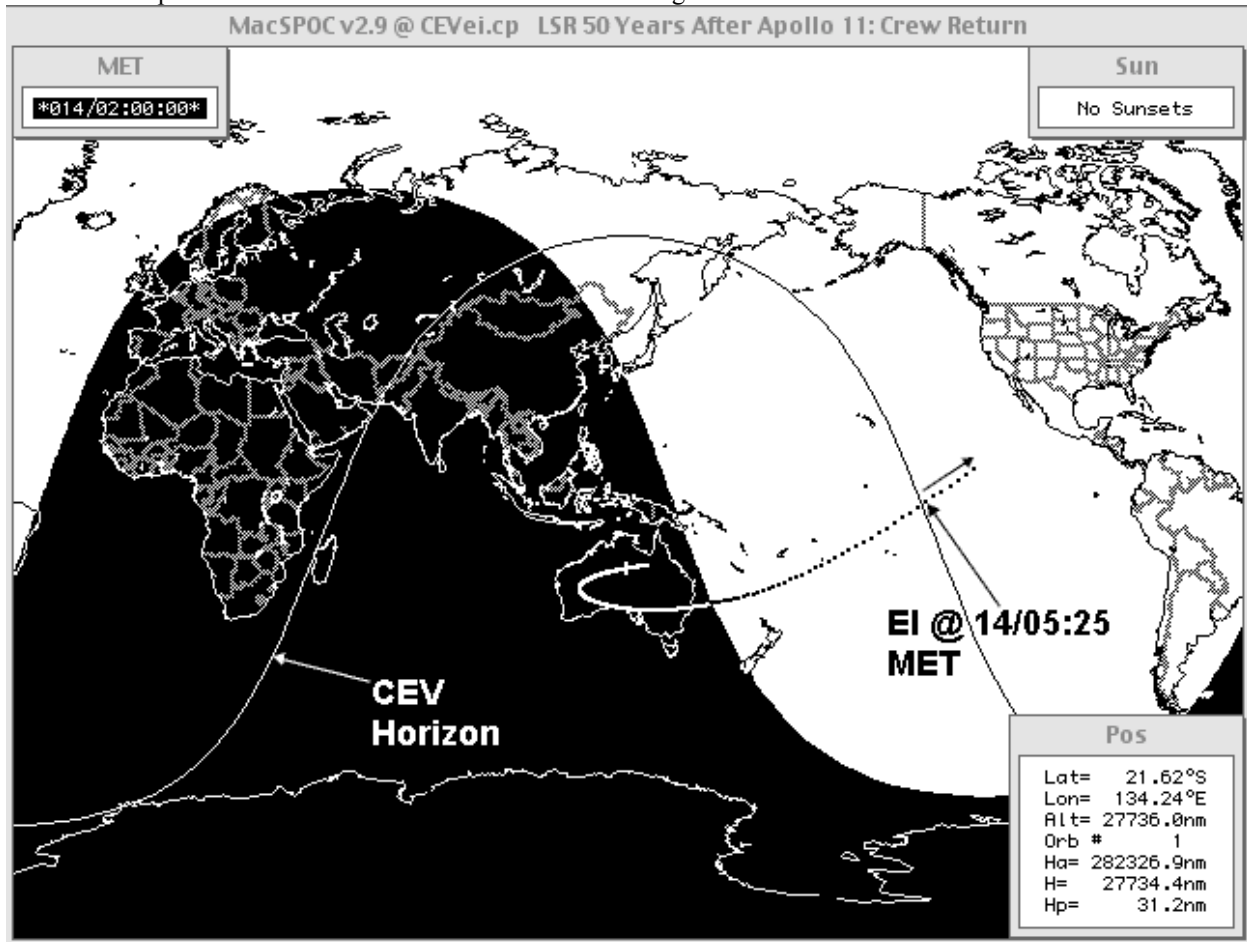


Figure 8: CEV Earth Return Ground Track

VIII. CEV/DM Trans-Lunar Abort Trajectories

The nominal CEV/DM trans-lunar trajectory design documented in Section VI approaches the Moon at high inclination to the lunar equator in order to achieve timely Aristarchus Plateau landing under GR&C #7 with a single in-plane LOI impulse. A consequence of this targeting strategy is departure from a coasted circumlunar trajectory providing Earth free return in the event of a trans-lunar abort. The same non-free return TLI targeting strategy was adopted for Apollo missions 15, 16, and 17 ([6], p. 1776 footnote). Although Apollo 13's TLI targeted Earth free return, nominal trans-lunar trajectory design required departing from this condition 28 hrs later ([6], p. 1780). Following mission abort, Apollo 13 required $\Delta v = 11.5$ m/s to reestablish free return 59 hrs after TLI ([6], p. 1777). To achieve Earth return in the primary Pacific Ocean recovery zone, Apollo 13 needed an additional $\Delta v = 262.3$ m/s 77 hrs after TLI and 2 hrs after circumlunar pericyynthion ([6], p. 1778).

Because Apollo 13 placed a premium on return to the prime recovery area, trans-lunar aborts documented in this section will do likewise under GR&C #20 by targeting $\lambda = -140^\circ$ at T_E . Unlike Apollo 13, this Earth return will be achieved in one abort impulse to facilitate Δv assessment for compliance with GR&C #21 and 22. Abort position,

together with initial velocity for the Δv assessment, are obtained from coasting CEV/DM post-TLI State #5 to each abort epoch.

Earth arrival boundary conditions for each trans-lunar abort are obtained using the same CSM T_E/δ iteration documented for TEI by Subsection A. In this case, trans-Earth departure is assumed to be near the nominal CEV/DM LOI epoch and is fixed on July 14 at 195/00:00 UTC. With respect to a nearly ideal 3-day trans-Earth transit imposing near-minimal trans-lunar abort Δv , two bracketing return condition sets arriving at $\lambda = -140^\circ$ arise from CSM-based T_E/δ iterations. These return conditions are summarized as follows.

Early Return: T_E on July 16 at 197/17:30 UTC; $\delta = +11.3^\circ$; $i = 29.375^\circ$

Late Return: T_E on July 17 at 198/17:46 UTC; $\delta = +13.8^\circ$; $i = 29.283^\circ$

With all boundary conditions determined, SPSM targeting of abort epoch velocity under GR&C #4 acceleration modeling is seeded with nominal trans-lunar velocity at the abort epoch unless otherwise noted. Computed trans-lunar abort Δv is then the SPSM velocity solution minus the nominal trans-lunar velocity. A series of trans-lunar abort epochs are assessed in chronologic order below.

The first abort epoch to be assessed is on July 11 at 192/00:00 UTC, 3 hrs after TLI. State #13 is the Early Return circumlunar SPSM solution.

State #13: CEV/DM post-trans-lunar Early Return circumlunar abort on 2019 July 11 at 192/00:00 UTC (abort $\Delta v = 111.070$ m/s; $H_p = +184.523$ km on July 13 at 194/17:38:34 UTC)

$$\mathbf{r} = \begin{bmatrix} -34158.659 \\ -35967.252 \\ -6223.572 \end{bmatrix} \text{ geocentric J2K km} \qquad \mathbf{v} = \begin{bmatrix} -1.517070 \\ -3.333627 \\ -1.066684 \end{bmatrix} \text{ geocentric J2K km/s}$$

$$i = 28.466^\circ \qquad u = 195.297^\circ \qquad \psi = 117.609^\circ \qquad \gamma = +69.271^\circ$$

Because Early Return circumlunar H_p is only apt to become unacceptably low as abort UTC becomes later, a Late Return circumlunar abort is also assessed at the first epoch to initiate trend data generation at the earliest practical time for this option. This SPSM solution appears as State #14.

State #14: CEV/DM post-trans-lunar Late Return circumlunar abort on 2019 July 11 at 192/00:00 UTC (abort $\Delta v = 102.773$ m/s; $H_p = +2817.164$ km on July 14 at 195/04:23:28 UTC)

$$\mathbf{r} = \begin{bmatrix} -34158.659 \\ -35967.252 \\ -6223.572 \end{bmatrix} \text{ geocentric J2K km} \qquad \mathbf{v} = \begin{bmatrix} -1.317161 \\ -3.373202 \\ -1.086292 \end{bmatrix} \text{ geocentric J2K km/s}$$

$$i = 26.623^\circ \qquad u = 196.297^\circ \qquad \psi = 115.693^\circ \qquad \gamma = +66.311^\circ$$

To illustrate geocentric geometry associated with circumlunar aborts, trajectories arising from State #13 (green) and #14 (blue) coasts to EI are co-plotted in Figure 9. Time ticks in this plot are annotated with UTC DOY = 192 to 198 = July 11 to 17. Dotted lines emanating from time ticks are projections onto the ecliptic plane. The shaded region of Earth's surface is in darkness.

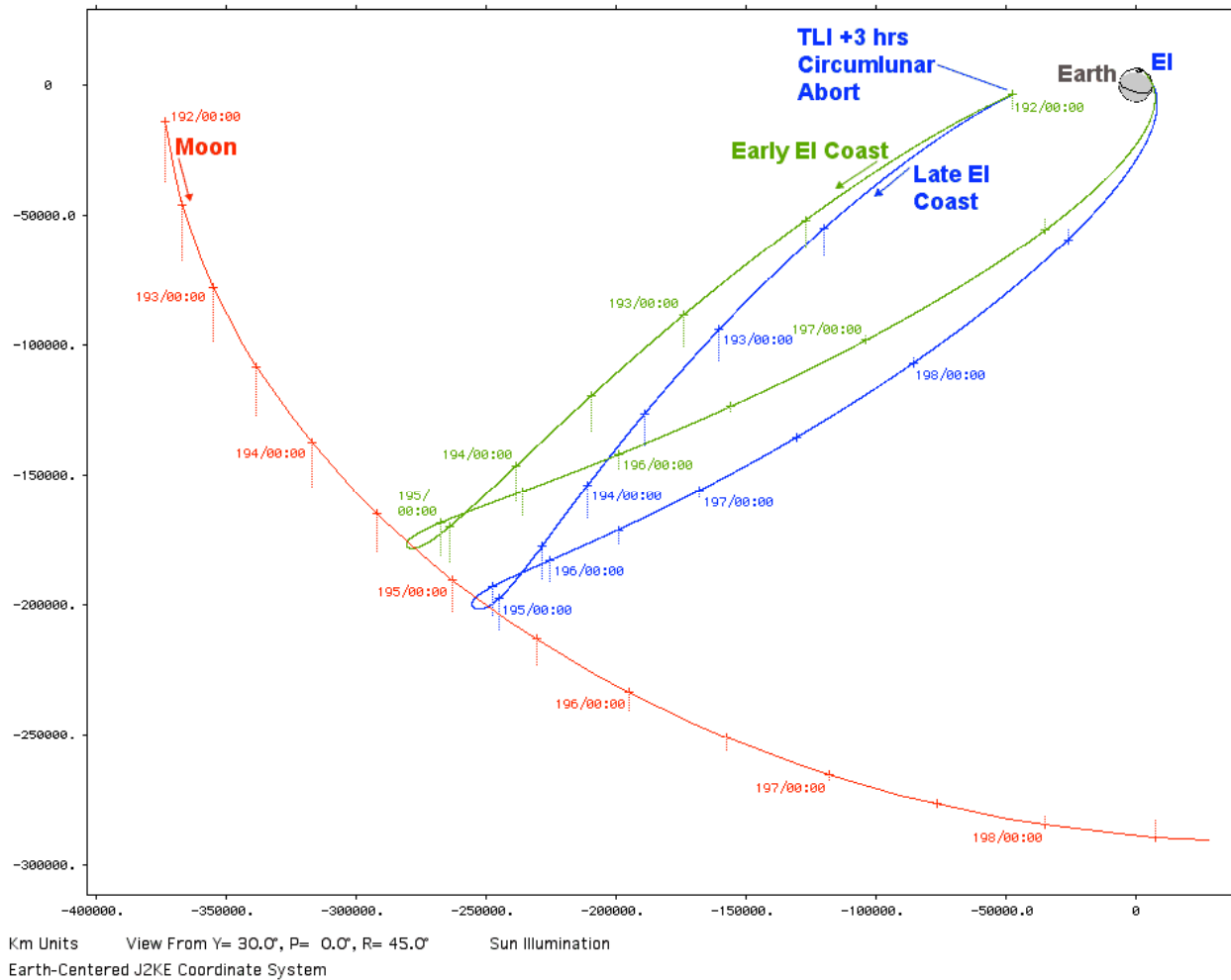


Figure 9: Two CEV/DM Circumlunar Abort Options At TLI +3 Hours

The second abort epoch to be assessed is on July 12 at 193/00:00 UTC, 27 hrs after TLI. State #15 is the Late Return circumlunar SPSM solution.

State #15: CEV/DM post-trans-lunar Late Return circumlunar abort on 2019 July 12 at 193/00:00 UTC (abort $\Delta v = 75.942$ m/s; $H_p = +2785.690$ km on July 14 at 195/03:05:50 UTC)

$$\mathbf{r} = \begin{bmatrix} -70642.807 \\ -197900.296 \\ -69199.664 \end{bmatrix} \text{ geocentric J2K km} \quad \mathbf{v} = \begin{bmatrix} -0.071687 \\ -1.308725 \\ -0.529229 \end{bmatrix} \text{ geocentric J2K km/s}$$

$$i = 24.286^\circ \quad u = 229.633^\circ \quad \psi = 106.291^\circ \quad \gamma = +74.057^\circ$$

Note that Late Return circumlunar abort Δv at this epoch is only 74% that of the corresponding abort 24 hrs earlier. This decrease is due to lower geocentric speed at the later abort epoch, facilitating the necessary course deviation from the nominal trajectory. This trend reverses later in trans-lunar flight because the course deviation becomes considerably larger.

The third abort epoch to be assessed is on July 13 at 194/00:00 UTC, 51 hrs after TLI. State #16 is the Late Return circumlunar SPSM solution.

State #16: CEV/DM post-trans-lunar Late Return circumlunar abort on 2019 July 13 at 194/00:00 UTC (abort $\Delta v = 88.162$ m/s; $H_p = +2662.139$ km on July 14 at 195/01:50:58 UTC)

$$\mathbf{r} = \begin{bmatrix} -76822.225 \\ -288606.069 \\ -108880.420 \end{bmatrix} \text{ geocentric J2K km} \quad \mathbf{v} = \begin{bmatrix} +0.061096 \\ -0.915671 \\ -0.364639 \end{bmatrix} \text{ geocentric J2K km/s}$$

$$i = 21.735^\circ \quad u = 247.835^\circ \quad \psi = 98.554^\circ \quad \gamma = +72.437^\circ$$

The fourth abort epoch to be assessed is on July 13 at 194/12:00 UTC, 63 hrs after TLI and 12 hrs before LOI. State #17 is the Late Return circumlunar SPSM solution.

State #17: CEV/DM post-trans-lunar Late Return circumlunar abort on 2019 July 13 at 194/12:00 UTC (abort $\Delta v = 166.965$ m/s; $H_p = +2366.599$ km on July 14 at 195/01:06:33 UTC)

$$\mathbf{r} = \begin{bmatrix} +47740.814 \\ +21483.713 \\ +1680.213 \end{bmatrix} \text{ selenocentric J2K km} \quad \mathbf{v} = \begin{bmatrix} -0.850457 \\ -0.538466 \\ -0.079129 \end{bmatrix} \text{ selenocentric J2K km/s}$$

$$i = 170.344^\circ \quad u = 287.457^\circ \quad \psi = 272.922^\circ \quad \gamma = -81.477^\circ$$

Because State #17 is such a large deviation from nominal lunar approach velocity, SPSM produces a retrograde Earth approach in violation of GR&C #19 when seeded with nominal departure velocity if Late Return boundary conditions are targeted. Consequently, SPSM first adopts State #16 coasted to $T_E -2$ hrs on July 17 at 198/15:46 UTC as arrival epoch and position. This solution then seeds SPSM to target the Late Return T_E and position, producing State #17.

The fifth and final abort epoch to be assessed is on July 13 at 194/18:00 UTC, 69 hrs after TLI and 6 hrs before LOI. State #18 is the Late Return circumlunar SPSM solution.

State #18: CEV/DM post-trans-lunar Late Return circumlunar abort on 2019 July 13 at 194/18:00 UTC (abort $\Delta v = 277.573$ m/s; $H_p = +1905.653$ km on July 14 at 195/00:40:08 UTC)

$$\mathbf{r} = \begin{bmatrix} +26194.323 \\ +12007.201 \\ -980.546 \end{bmatrix} \text{ selenocentric J2K km} \quad \mathbf{v} = \begin{bmatrix} -0.860899 \\ -0.647201 \\ -0.030738 \end{bmatrix} \text{ selenocentric J2K km/s}$$

$$i = 166.082^\circ \quad u = 292.062^\circ \quad \psi = 275.318^\circ \quad \gamma = -77.182^\circ$$

The State #18 SPSM solution is unable to use nominal CEV/DM velocity at the abort epoch as a seed. As with the State #17 solution, seeding is from an SPSM solution targeting coasted State #16 $T_E -2$ hrs arrival conditions from the 18:00 UTC abort epoch.

The significant course deviation required by the State #18 abort is illustrated by Figure 10, in which State #18 (green) and #5 (blue) coasts from the abort epoch are co-plotted. Time ticks in this plot are annotated with UTC DOY = 194 to 195 = July 13 to 14. Dotted lines emanating from time ticks are projections onto the lunar equator plane. Shaded points of the Moon's surface are located on its farside from Earth. The Figure 10 plot is viewed from a perspective very nearly normal to the State #5 trajectory coast. Note the nominal trajectory would deviate from the Figure 10 (blue) plot at pericynthion, where LOI establishes a circular LLO with H = 100 km.

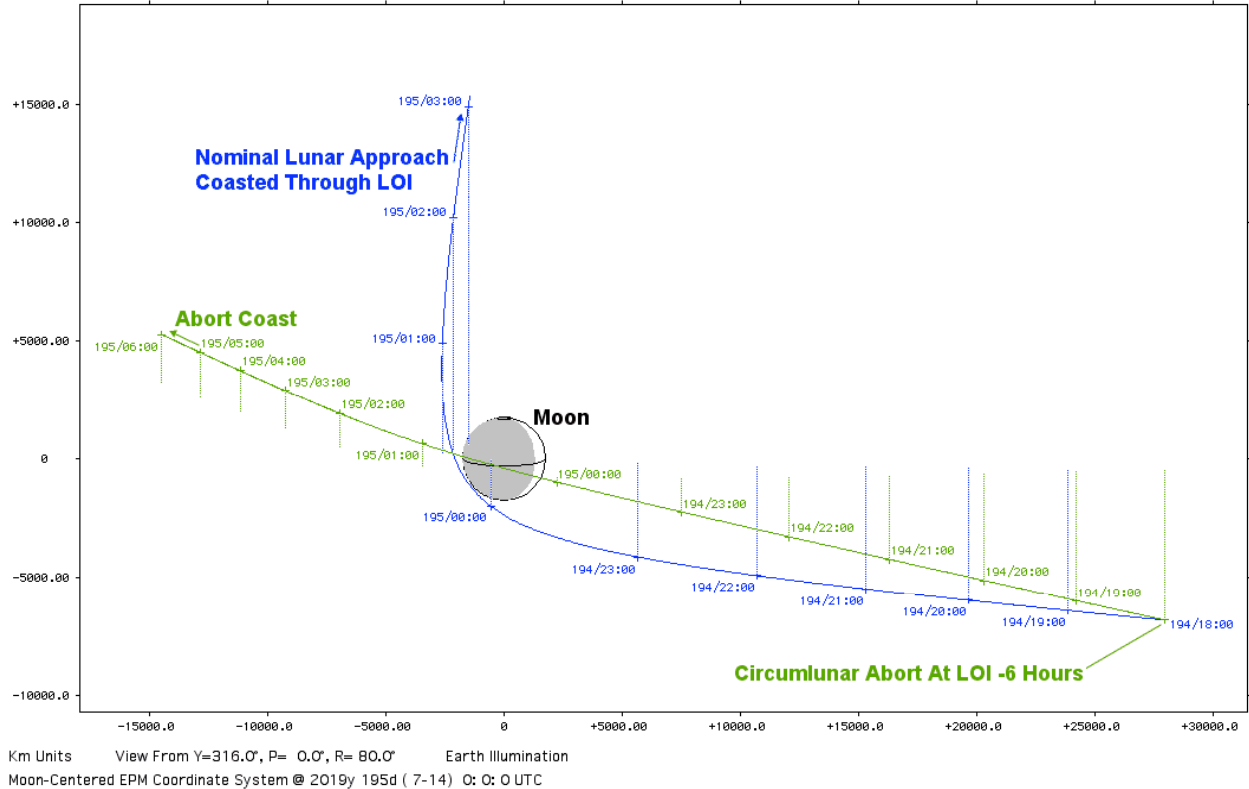


Figure 10: Circumlunar Late Return Abort At LOI -6 Hours

The abort epoch on July 13 at 194/18:00 UTC is also assessed for Early Return boundary conditions. As expected, this circumlunar option is unacceptable because the coasted abort trajectory has $H_p < 0$. Nevertheless, the State #19 "solution" is included for academic interest. It is obtained by seeding SPSM with nominal velocity at the abort epoch.

State #19: CEV/DM post-trans-lunar Early Return circumlunar abort on 2019 July 13 at 194/18:00 UTC (abort $\Delta v = 275.995$ m/s; $H_p = -313.315$ km on July 13 at 194/23:20:51 UTC)

$$\mathbf{r} = \begin{bmatrix} +26194.323 \\ +12007.201 \\ -980.546 \end{bmatrix} \text{ selenocentric J2K km} \quad \mathbf{v} = \begin{bmatrix} -1.147856 \\ -0.675924 \\ -0.003096 \end{bmatrix} \text{ selenocentric J2K km/s}$$

$$i = 166.969^\circ \quad u = 278.637^\circ \quad \psi = 271.991^\circ \quad \gamma = -83.777^\circ$$

As at all other trans-lunar abort epochs assessed, a "direct" option exists on July 13 at 194/18:00 UTC. Because this abort option nearly halts Moonward motion, it is not circumlunar and entails relatively large Δv compared to such aborts. The State #20 solution attempts to minimize abort Δv by targeting Late Return boundary conditions. This is accomplished by seeding SPSM with a selenocentric velocity opposed to that of the nominal trajectory at the abort epoch.

State #20: CEV/DM post-trans-lunar Late Return direct abort on 2019 July 13 at 194/18:00 UTC (abort $\Delta v = 1236.895$ m/s; $H_p = +24837.614$ km on July 13 at 194/21:20:35 UTC)

$$\mathbf{r} = \begin{bmatrix} +26194.323 \\ +12007.201 \\ -980.546 \end{bmatrix} \text{ selenocentric J2K km} \quad \mathbf{v} = \begin{bmatrix} -0.700696 \\ +0.686313 \\ +0.225881 \end{bmatrix} \text{ selenocentric J2K km/s}$$

$$i = 15.302^\circ \quad u = 237.639^\circ \quad \psi = 98.331^\circ \quad \gamma = -20.864^\circ$$

To summarize, CEV/DM circumlunar aborts returning to Earth with nominal EI conditions specified by GR&C #19 and #20 can be performed with $\Delta v < 300$ m/s throughout the interval from TLI +3 hrs to LOI -6 hrs. These aborts are well within DM and SM propulsive budgets specified by GR&C #21 and #22, respectively. Circumlunar abort Δv necessary to achieve Late Return arrival conditions is plotted as a function of abort time in Figure 11. When adequate H_p renders them practical, Early Return circumlunar aborts require Δv differing from corresponding Late Return aborts by only a few m/s.

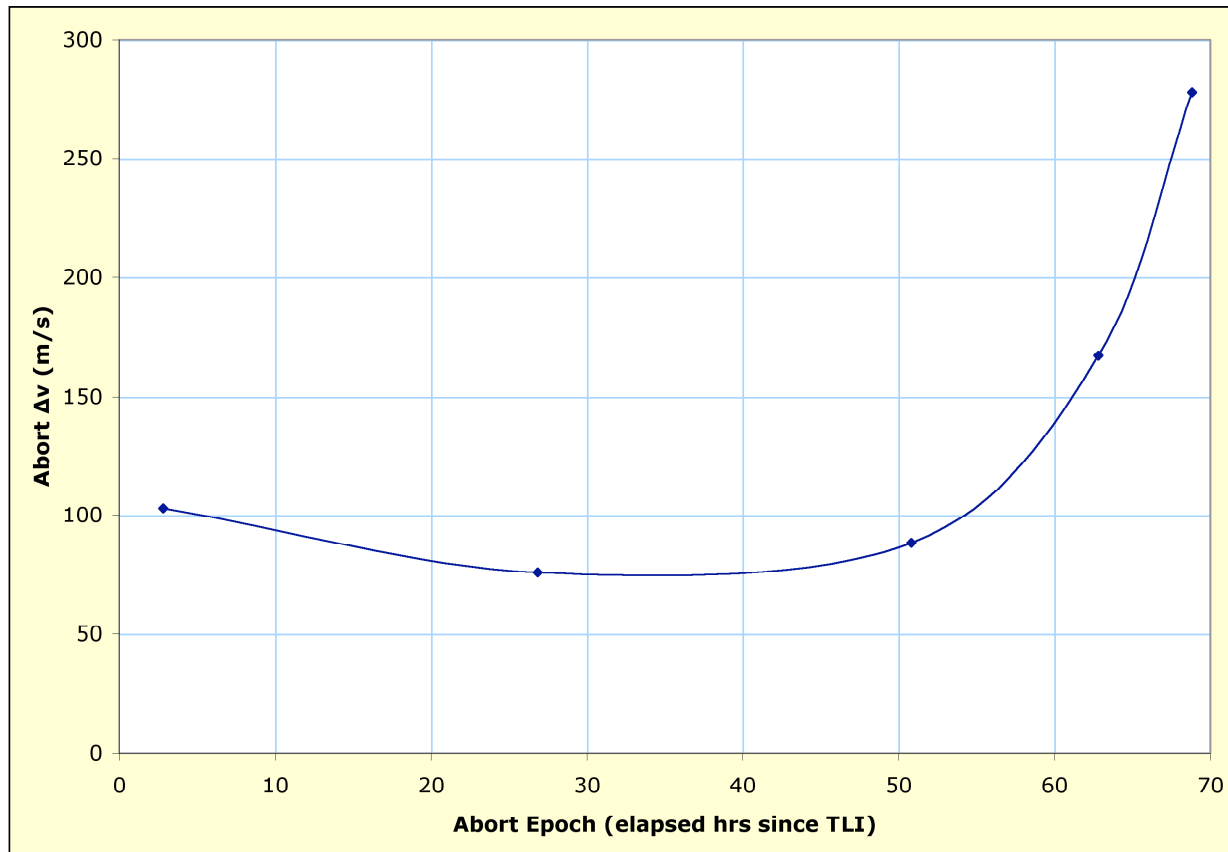


Figure 11: CEV/DM Trans-Lunar Abort Δv ($T_E = \text{July 17 at 198/17:46 UTC}$)

IX. CEV/DM Post-LOI Abort Trajectories From LLO

Previous study of Earth return from polar LLO [11] has devised a two-impulse targeting strategy known as TEI+HCI. With CEV/DM inclination only 12.9° from polar following nominal LOI, TEI+HCI concepts are readily applied to LLO aborts on this mission. The first TEI+HCI impulse is coplanar to the greatest extent possible with the initial LLO. This initial impulse is called TEI because it produces lunar escape and Earth return without further propulsion. Coasted transit time from TEI to T_E is strongly influenced by polar LLO nodal longitudes on the Moon's equator at TEI. If the polar LLO has an ascending or descending node on the Moon's nearside western hemisphere, as does the CEV/DM following nominal LOI (see Figure 5), transit time decreases as this node shifts westward toward -90° with lunar rotation. If propulsive capability permits, a second hybrid course insertion (HCI) impulse, containing a dominant Δv component directed at Earth, may be used to shift T_E earlier as required. Although HCI performance in shifting T_E per unit Δv is rather insensitive to the coast interval from TEI to HCI, ~ 6 hrs is nearly optimal. With HCI scheduled some 6 hrs after TEI imparts lunar escape, geocentric speed is nearly minimal, and a large course deviation significantly shortening trans-Earth coast requires less Δv than would be the case in polar LLO.

Targeting any TEI+HCI abort entails a process very similar to that associated with a nominal TEI, and it commences with geocentric short-way CSM T_E/δ iterations. An appropriate CSM departure epoch is fixed based on the abort scenario. Approximate CSM departure selenocentric position is fixed at $H = +100$ km, $\lambda = 0$, and $\delta = 0$.

Arrival epoch T_E is initially iterated with CSM to an epoch consistent with the GR&C #18 trans-Earth coast interval. Following T_E/δ iterations, CSM selenocentric departure velocity is input to POM as lunar escape asymptotic velocity. Serving as a "no earlier than" threshold for TEI, POM's "launch" (departure) UTC is set to an epoch near that used for CSM T_E/δ iterations. Nominal post-LOI State #6 is coasted to this epoch to supply a POM departure position. In a TEI+HCI abort context, POM solutions deviate from GR&C #6 and #16 because time to coast from departure to arrival at TEI is specified as less than one orbit. The POM solution's arrival UTC then becomes a preliminary TEI epoch returning CEV to Earth at T_E . Next, the POM solution's departure ψ is subtracted from nominal LLO ψ at the same epoch to verify the POM arc is sufficiently coplanar with the nominal orbit plane coasted from LOI. This $\Delta\psi$ targeting residual has a magnitude quantifying the degree to which TEI Δv is not coplanar with the post-LOI orbit. If $\Delta\psi$ magnitude is not minimal, CSM T_E/δ iterations are resumed with T_E incremented by a day. When a POM solution nearly coplanar with the nominal LLO is obtained, its departure epoch and velocity are used to seed a precision TEI solution using SPSM with GR&C #4 accelerations.

A cautionary note is in order regarding the POM departure position selected in a TEI+HCI context. Because there is no launch location or exact UTC constraining this position, the associated POM departure epoch to which State #6 is coasted could yield virtually any selenocentric POM departure δ in this mission's nearly polar LLO. In POM, the State #6 coasted position and the CSM selenocentric asymptotic departure velocity are necessary to define the LLO plane leading to TEI. As T_E is incremented to achieve small $\Delta\psi$ magnitudes, the CSM departure velocity will likewise become nearly *coplanar* with the State #6 coasted LLO as a matter of design. In this process, CSM departure velocity must not also become nearly *co-linear* with the coasted State #6 position, or POM will be unable to accurately compute the LLO plane leading to TEI. Extreme cases, in which co-linearity is within 5° , can produce $\Delta\psi$ magnitude in excess of 160° just as a nearly zero value is expected. In practice, this co-linearity condition is easily avoided because CSM departure velocity will always possess a low-magnitude selenocentric δ . For the nearly polar LLO in this mission, co-linearity is avoided by coasting State #6 to nearly polar δ . A similar avoidance strategy can be devised for low inclination LLO by coasting the nominal trajectory to a selenocentric λ nearly 90° from the departure velocity λ . Limited experience with POM in the TEI+HCI application indicates deviation from co-linearity by more than 10° is sufficient to compute an accurate plane leading to TEI.

C. LLO #1 TEI+HCI Abort

Shortly after nominal LOI on July 14 at 195/00:08:40 UTC, CEV/DM undergoes an ascending node passage on the Moon's farside equator, and LLO #1 begins. The initial TEI+HCI abort opportunity during LLO #1 is informally known as a lunar orbit touch-and-go (LOTAG). A preliminary trans-Earth departure epoch for geocentric CSM T_E/δ iterations is fixed about midway through LLO #1 at 01:00 UTC. The departure epoch and selenocentric position pertaining to POM targeting are fixed before LLO #1 at nominal LOI (see State #6 **r**) as a matter of convenience^{§§}, but this selection still leads to POM arrival and TEI epochs during LLO #1. Per State #6, nominal $\psi = 343.759^\circ$ at the POM departure epoch. Table 2 summarizes T_E/δ iteration results, together with associated POM $\Delta\psi$ assessments.

Table 2: CSM T_E/δ Solutions And POM $\Delta\psi$ Assessments Supporting LLO #1 TEI+HCI Abort

T_E UTC Date	T_E UTC	Arrival δ	Arrival ψ	Arrival γ	Arrival i	$\Delta\psi$
July 17	198/17:48	+13.8°	63.857°	-5.832°	29.333°	+63.301°
July 18	199/17:56	+15.3°	65.012°	-5.860°	29.041°	+48.805°
July 19	200/18:01	+16.0°	64.195°	-5.850°	30.071°	+36.205°
July 20	201/18:03	+16.7°	64.708°	-5.859°	30.002°	+25.640°
July 21	202/18:04	+17.4°	66.066°	-5.787°	29.286°	+17.146°
July 22	203/18:04	+17.7°	65.457°	-5.779°	29.935°	+10.724°
July 23	204/18:03	+18.0°	65.523°	-5.788°	30.050°	+5.583°
July 24	205/18:02	+18.3°	65.585°	-5.732°	30.172°	+1.476°
July 25	206/18:00	+18.6°	66.803°	-5.734°	29.408°	-2.663°

^{§§} Nominal LOI **r** is at selenocentric $\delta = -36.891^\circ$. This is sufficiently removed from low-declination selenocentric asymptotic CSM departure velocity to insure an accurate POM plane in LLO can be defined.

By virtue of its minimal $\Delta\psi$ magnitude, the July 24 CSM/POM solution and associated boundary conditions seed SPSM first. Unfortunately, the SPSM solution post-TEI has $\Delta\psi = +3.419^\circ$ with respect to the nominal LLO at that epoch. This deviation from CSM/POM expectations is due to the presence of GR&C #4 accelerations in SPSM trajectories, and it suggests seeding SPSM with the July 25 CSM/POM solution. From this action, an SPSM TEI solution is obtained with $\Delta\psi = +0.251^\circ$. The associated post-TEI State #21 appears below.

State #21: CEV/DM LLO #1 TEI+HCI abort post-TEI on 2019 July 14 at 195/01:36:45 UTC (TEI $\Delta v = 902.703$ m/s; coasted EI geocentric speed = 11.008 km/s on July 25 at 206/17:59:38 UTC)

$$\mathbf{r} = \begin{bmatrix} +1214.317 \\ +733.270 \\ -1167.850 \end{bmatrix} \text{ selenocentric J2K km} \quad \mathbf{v} = \begin{bmatrix} -1.566787 \\ -0.385556 \\ -1.955359 \end{bmatrix} \text{ selenocentric J2K km/s}$$

$$i = 102.765^\circ \quad u = 231.147^\circ \quad \psi = 199.857^\circ \quad \gamma = +1.209^\circ$$

State #21 is coasted to July 14 at 195/08:00 UTC, the notional HCI epoch. To initiate HCI targeting, the coast's terminal conditions become departure epoch and position for another CSM T_E/δ iteration. Although any Table 2 UTC date prior to July 25 could be targeted by this iteration as T_E , July 18 is selected as illustrative. The associated CSM solution has T_E on July 18 at 199/17:50 UTC with geocentric arrival parameters $\delta = +15.3^\circ$, $\psi = 64.101^\circ$, $\gamma = -5.782^\circ$, and $i = 29.810^\circ$. With this CSM solution serving as initial seed to SPSM, the State #22 HCI solution results. Note HCI Δv is directed within 3° of the geocenter, and its Earthward component is 882.121 m/s.

State #22: CEV/DM LLO #1 TEI+HCI abort post-HCI on 2019 July 14 at 195/08:00 UTC (HCI $\Delta v = 883.043$ m/s; coasted EI geocentric speed = 10.994 km/s on July 18 at 199/17:49:45 UTC)

$$\mathbf{r} = \begin{bmatrix} -27773.250 \\ -11226.271 \\ -7723.606 \end{bmatrix} \text{ selenocentric J2K km} \quad \mathbf{v} = \begin{bmatrix} -0.939986 \\ +0.348664 \\ +0.164763 \end{bmatrix} \text{ selenocentric J2K km/s}$$

$$i = 173.513^\circ \quad u = 328.926^\circ \quad \psi = 275.563^\circ \quad \gamma = +41.726^\circ$$

Figure 12 illustrates coasted geocentric trajectories initiated by State #21 (green) and #22 (blue). Both plots end at their respective EI epochs. Time ticks in this plot are annotated with UTC DOY = 196 to 206 = July 15 to 25. Dotted lines emanating from time ticks are projections onto the ecliptic plane. The shaded region of Earth's surface is in darkness.

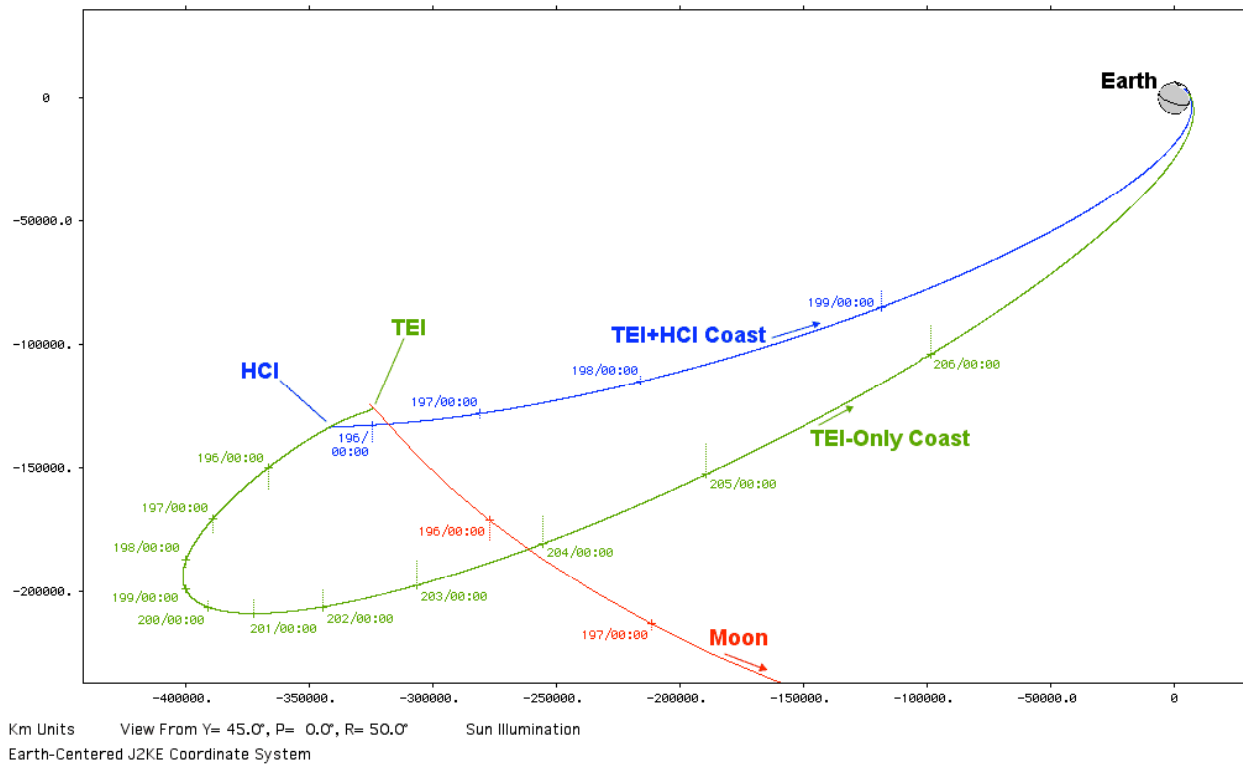


Figure 12: LLO #1 TEI+HCI Abort Trajectories

If the LLO #1 TEI+HCI abort scenario is performed entirely with DM propulsion, expended $\Delta v = 874.668$ m/s (nominal LOI) + 902.703 m/s (TEI) + 883.043 m/s (HCI) = 2660.414 m/s, leaving a DM margin of +355 m/s with respect to GR&C #21. Consequently, if DM propulsion is functional throughout this scenario, no deterministic CEV impulses are required to achieve Earth arrival 4.7 days after nominal LOI (Figure 12's blue trajectory). If DM propulsion is totally disabled after nominal LOI, an intact CEV has propulsive capability to perform the LLO #1 TEI impulse with +4 m/s of margin in its SM under GR&C #22, assuming prior DM jettison. This scenario results in Earth arrival 11.7 days after nominal LOI (Figure 12's green trajectory) without any HCI. If the DM only has TEI propulsive capability after a nominal LOI, it can be jettisoned before an intact CEV performs the HCI impulse with +24 m/s margin in its SM to achieve Earth arrival 4.7 days after nominal LOI.

D. LLO #9 TEI+HCI Abort

On July 14 at 195/16:33 UTC, about 20 min prior to the backup landing opportunity at Aristarchus Plateau (see Figure 5), coasted CEV/DM LLO motion following nominal LOI is near its most northerly selenocentric position during LLO #9. This epoch and position at selenocentric $\delta = +77.091^\circ$ become POM departure boundary conditions for a second notional TEI+HCI abort initiated later in LLO #9. Nominal post-LOI coast produces $\psi = 268.619^\circ$ at the POM departure epoch. A trans-Earth departure epoch for geocentric CSM T_E/δ iterations is fixed about midway through LLO #9 at 195/17:00 UTC. Table 3 summarizes T_E/δ iteration results, together with associated POM $\Delta\psi$ assessments.

Table 3: CSM T_E/δ Solutions And POM $\Delta\psi$ Assessments Supporting LLO #9 TEI+HCI Abort

T_E UTC Date	T_E UTC	Arrival δ	Arrival ψ	Arrival γ	Arrival i	$\Delta\psi$
July 17	198/18:11	+13.8°	63.834°	-5.804°	29.354°	-70.272°
July 18	199/18:25	+15.3°	62.975°	-5.801°	30.769°	-48.347°
July 19	200/18:31	+16.8°	64.917°	-5.826°	29.884°	-30.406°
July 20	201/18:35	+17.6°	65.101°	-5.786°	30.164°	-17.660°
July 21	202/18:36	+18.2°	65.836°	-5.853°	29.919°	-8.861°
July 22	203/18:37	+18.6°	65.359°	-5.798°	30.519°	-2.738°
July 23	204/18:36	+19.0°	66.256°	-5.845°	30.062°	+1.805°

By virtue of its minimal $\Delta\psi$ magnitude, the July 23 CSM/POM solution serves to seed SPSM TEI targeting with GR&C #4 accelerations invoked. From this action, an SPSM TEI solution is obtained with $\Delta\psi = +0.258^\circ$. The associated post-TEI State #23 appears below.

State #23: CEV/DM LLO #9 TEI+HCI abort post-TEI on 2019 July 14 at 195/17:17:15 UTC (TEI $\Delta v = 864.801$ m/s; coasted EI geocentric speed = 11.000 km/s on July 23 at 204/18:35:33 UTC)

$$\mathbf{r} = \begin{bmatrix} +1322.072 \\ +759.844 \\ -1025.112 \end{bmatrix} \text{ selenocentric J2K km} \quad \mathbf{v} = \begin{bmatrix} -1.397618 \\ -0.319178 \\ -2.045984 \end{bmatrix} \text{ selenocentric J2K km/s}$$

$$i = 103.085^\circ \quad u = 225.598^\circ \quad \psi = 198.376^\circ \quad \gamma = +0.088^\circ$$

State #23 is coasted to July 14 at 195/23:15 UTC, the notional HCI epoch. To initiate HCI targeting, the coast's terminal conditions become departure epoch and position for another CSM T_E/δ iteration. Although any Table 3 UTC date prior to July 23 could be targeted by this iteration as T_E , July 18 is selected for comparison with LLO #1 TEI+HCI. The associated CSM solution has T_E on July 18 at 199/18:16 UTC with geocentric arrival parameters $\delta = +15.8^\circ$, $\psi = 64.322^\circ$, $\gamma = -5.816^\circ$, and $i = 29.866^\circ$. With this CSM solution serving as initial seed to SPSM, the State #24 HCI solution results. Note HCI Δv is directed within 2° of the geocenter, and its Earthward component is 936.496 m/s.

State #24: CEV/DM LLO #9 TEI+HCI abort post-HCI on 2019 July 14 at 195/23:15 UTC (HCI $\Delta v = 936.704$ m/s; coasted EI geocentric speed = 10.999 km/s on July 18 at 199/18:15:49 UTC)

$$\mathbf{r} = \begin{bmatrix} -24617.196 \\ -9994.372 \\ -7906.374 \end{bmatrix} \text{ selenocentric J2K km} \quad \mathbf{v} = \begin{bmatrix} -0.977543 \\ +0.426345 \\ +0.191309 \end{bmatrix} \text{ selenocentric J2K km/s}$$

$$i = 172.063^\circ \quad u = 318.242^\circ \quad \psi = 275.938^\circ \quad \gamma = +37.517^\circ$$

Because HCI Δv associated with July 18 Earth arrival exceeds SM capability specified by GR&C #22, an alternative HCI solution is sought with Earth arrival on July 19. The associated CSM solution has T_E on July 19 at 200/18:24 UTC with geocentric arrival parameters $\delta = +17.1^\circ$, $\psi = 64.967^\circ$, $\gamma = -5.885^\circ$, and $i = 30.002^\circ$. With this CSM solution serving as initial seed to SPSM, the State #25 HCI solution results. Note HCI Δv is directed within 3° of the geocenter, and its Earthward component is 601.410 m/s.

State #25: CEV/DM LLO #9 TEI+HCI abort post-HCI on 2019 July 14 at 195/23:15 UTC (HCI $\Delta v = 602.061$ m/s; coasted EI geocentric speed = 10.991 km/s on July 19 at 200/18:23:46 UTC)

$$\mathbf{r} = \begin{bmatrix} -24617.196 \\ -9994.372 \\ -7906.374 \end{bmatrix} \text{ selenocentric J2K km} \quad \mathbf{v} = \begin{bmatrix} -1.006711 \\ +0.118519 \\ +0.061910 \end{bmatrix} \text{ selenocentric J2K km/s}$$

$$i = 167.702^\circ \quad u = 334.420^\circ \quad \psi = 281.124^\circ \quad \gamma = +55.172^\circ$$

Figure 13 illustrates coasted geocentric trajectories initiated by State #23 (green) and #25 (blue). Both plots end at their respective EI epochs. Time ticks in this plot are annotated with UTC DOY = 196 to 204 = July 15 to 23. Dotted lines emanating from time ticks are projections onto the ecliptic plane. The shaded region of Earth's surface is in darkness.

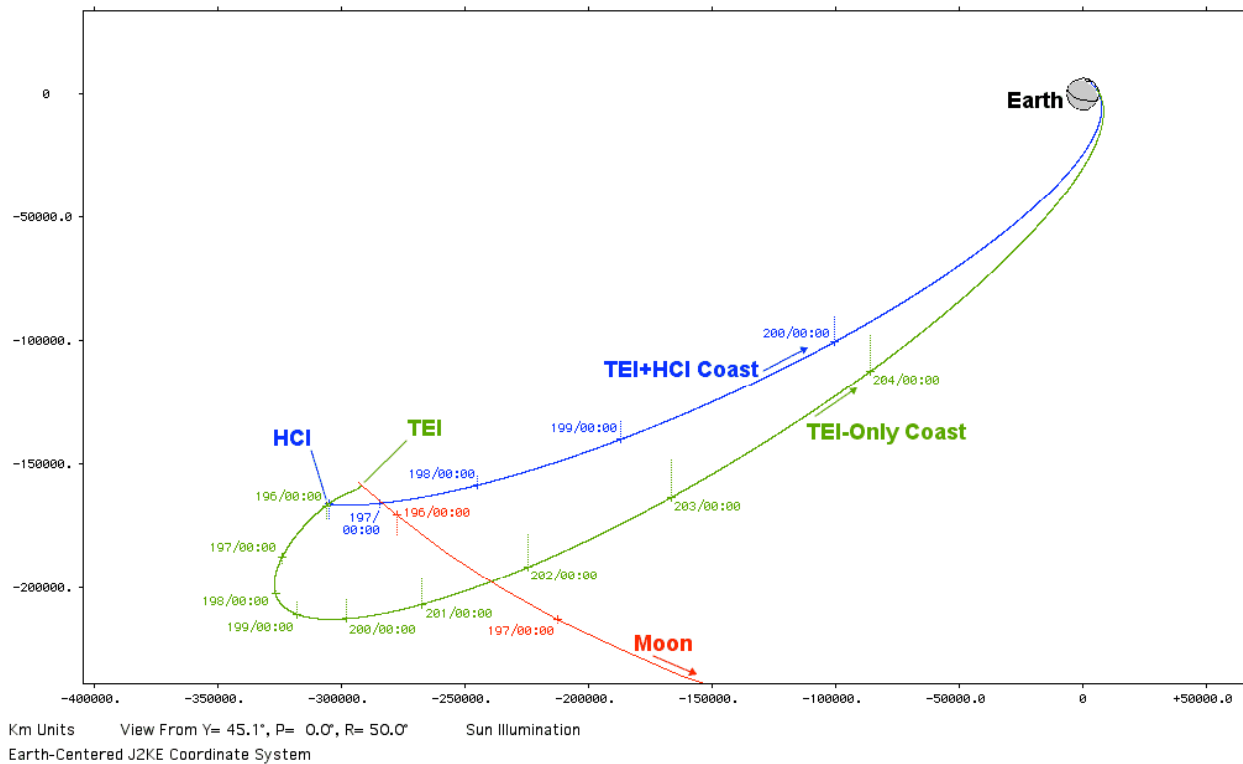


Figure 13: LLO #9 TEI+HCI Abort Trajectories

If the LLO #9 TEI+HCI abort scenario with Earth arrival on July 18 is performed entirely with DM propulsion, expended $\Delta v = 874.668$ m/s (nominal LOI) + 864.801 m/s (TEI) + 936.704 m/s (HCI) = 2676.173 m/s, leaving a DM margin of +339 m/s with respect to GR&C #21. Consequently, if DM propulsion is functional throughout this scenario, no deterministic CEV impulses are required to achieve Earth arrival 4.8 days after nominal LOI. If DM propulsion is totally disabled after nominal LOI, an intact CEV has propulsive capability to perform the LLO #9 TEI impulse for Earth arrival on July 23 with +42 m/s of margin in its SM under GR&C #22, assuming prior DM jettison. This scenario results in Earth arrival 9.8 days after nominal LOI (Figure 13's green trajectory) without any HCI. If the DM only has TEI propulsive capability after a nominal LOI and is jettisoned before HCI, an intact CEV would possess a margin of -30 m/s in its SM with respect to performing the HCI achieving July 18 Earth arrival.

To address the SM capability shortfall with respect to a July 18 Earth arrival HCI, a viable alternative with respect to GR&C #22 is provided when arrival is postponed to July 19. The one-day Earth arrival delay reduces HCI Δv by 36% to 602.061 m/s. Assuming DM performs LLO #9 TEI and is jettisoned before HCI, SM margin with respect to the reduced HCI impulse is +305 m/s. This TEI+HCI option achieves Earth arrival 5.8 days after nominal LOI (Figure 13's blue trajectory).

E. LLO #21 TEI+HCI Abort

On July 15 at 196/16:06 UTC, about a day after the backup landing opportunity at Aristarchus Plateau (see Figure 5), coasted CEV/DM LLO motion following nominal LOI is near its most northerly selenocentric position during LLO #21. This epoch and position at selenocentric $\delta = +77.056^\circ$ become POM departure boundary conditions for a third notional TEI+HCI abort initiated later in LLO #21. Nominal post-LOI coast produces $\psi = 275.435^\circ$ at the POM departure epoch. A trans-Earth departure epoch for geocentric CSM T_E/δ iterations is fixed about midway through LLO #21 at 196/17:00 UTC. Table 4 summarizes T_E/δ iteration results, together with associated POM $\Delta\psi$ assessments.

Table 4: CSM T_E/δ Solutions And POM $\Delta\psi$ Assessments Supporting LLO #21 TEI+HCI Abort

T_E UTC Date	T_E UTC	Arrival δ	Arrival ψ	Arrival γ	Arrival i	$\Delta\psi$
July 18	199/19:00	+14.9°	64.551°	-5.834°	29.237°	-57.632°
July 19	200/19:14	+16.4°	64.047°	-5.810°	30.394°	-36.020°
July 20	201/19:20	+17.7°	65.448°	-5.874°	29.943°	-18.374°
July 21	202/19:24	+18.5°	65.802°	-5.832°	30.117°	-5.792°
July 22	203/19:26	+19.1°	66.125°	-5.794°	30.221°	+2.906°

By virtue of its minimal $\Delta\psi$ magnitude, the July 22 CSM/POM solution serves to seed SPSM TEI targeting with GR&C #4 accelerations invoked. From this action, an SPSM TEI solution is obtained with $\Delta\psi = -2.411^\circ$. The associated post-TEI State #26 appears below.

State #26: CEV/DM LLO #21 TEI+HCI abort post-TEI on 2019 July 15 at 196/16:49:25 UTC (TEI $\Delta v = 837.611$ m/s; coasted EI geocentric speed = 10.994 km/s on July 22 at 203/19:25:26 UTC)

$$\mathbf{r} = \begin{bmatrix} +1392.608 \\ +774.821 \\ -914.522 \end{bmatrix} \text{ selenocentric J2K km} \quad \mathbf{v} = \begin{bmatrix} -1.211253 \\ -0.324806 \\ -2.124318 \end{bmatrix} \text{ selenocentric J2K km/s}$$

$$i = 104.686^\circ \quad u = 221.839^\circ \quad \psi = 199.381^\circ \quad \gamma = +0.054^\circ$$

State #26 is coasted to July 15 at 196/23:00 UTC, the notional HCI epoch. To initiate HCI targeting, the coast's terminal conditions become departure epoch and position for another CSM T_E/δ iteration. Although any Table 4 UTC date prior to July 22 could be targeted by this iteration as T_E , July 18 is selected for comparison with LLO #1 and #9 TEI+HCI. The associated CSM solution has T_E on July 18 at 199/18:49 UTC with geocentric arrival parameters $\delta = +14.9^\circ$, $\psi = 64.044^\circ$, $\gamma = -5.800^\circ$, and $i = 29.669^\circ$. With this CSM solution serving as initial seed to SPSM, the State #27 HCI solution results. Note HCI Δv is directed within 2° of the geocenter, and its Earthward component is 1243.122 m/s.

State #27: CEV/DM LLO #21 TEI+HCI abort post-HCI on 2019 July 15 at 196/23:00 UTC (HCI $\Delta v = 1243.588$ m/s; coasted EI geocentric speed = 11.028 km/s on July 18 at 199/18:48:54 UTC)

$$\mathbf{r} = \begin{bmatrix} -23745.705 \\ -10324.592 \\ -8694.150 \end{bmatrix} \text{ selenocentric J2K km} \quad \mathbf{v} = \begin{bmatrix} -1.093942 \\ +0.701889 \\ +0.314354 \end{bmatrix} \text{ selenocentric J2K km/s}$$

$$i = 171.823^\circ \quad u = 305.674^\circ \quad \psi = 274.790^\circ \quad \gamma = +25.974^\circ$$

Because HCI Δv associated with July 18 Earth arrival exceeds SM capability specified by GR&C #22, an alternative HCI solution is sought with Earth arrival on July 19. The associated CSM solution has T_E on July 19 at 200/19:05 UTC with geocentric arrival parameters $\delta = +16.9^\circ$, $\psi = 64.592^\circ$, $\gamma = -5.837^\circ$, and $i = 30.201^\circ$. With this CSM solution serving as initial seed to SPSM, the State #28 HCI solution results. Note HCI Δv is directed within 1° of the geocenter, and its Earthward component is 709.509 m/s.

State #28: CEV/DM LLO #21 TEI+HCI abort post-HCI on 2019 July 15 at 196/23:00 UTC (HCI $\Delta v = 709.585$ m/s; coasted EI geocentric speed = 10.998 km/s on July 19 at 200/19:04:51 UTC)

$$\mathbf{r} = \begin{bmatrix} -23745.705 \\ -10324.592 \\ -8694.150 \end{bmatrix} \text{ selenocentric J2K km} \quad \mathbf{v} = \begin{bmatrix} -1.046062 \\ +0.216191 \\ +0.096236 \end{bmatrix} \text{ selenocentric J2K km/s}$$

$$i = 168.281^\circ \quad u = 325.330^\circ \quad \psi = 279.682^\circ \quad \gamma = +48.003^\circ$$

Figure 14 illustrates coasted geocentric trajectories initiated by State #26 (green) and #28 (blue). Both plots end at their respective EI epochs. Time ticks in this plot are annotated with UTC DOY = 197 to 203 = July 16 to 22. Dotted lines emanating from time ticks are projections onto the ecliptic plane. The shaded region of Earth's surface is in darkness.

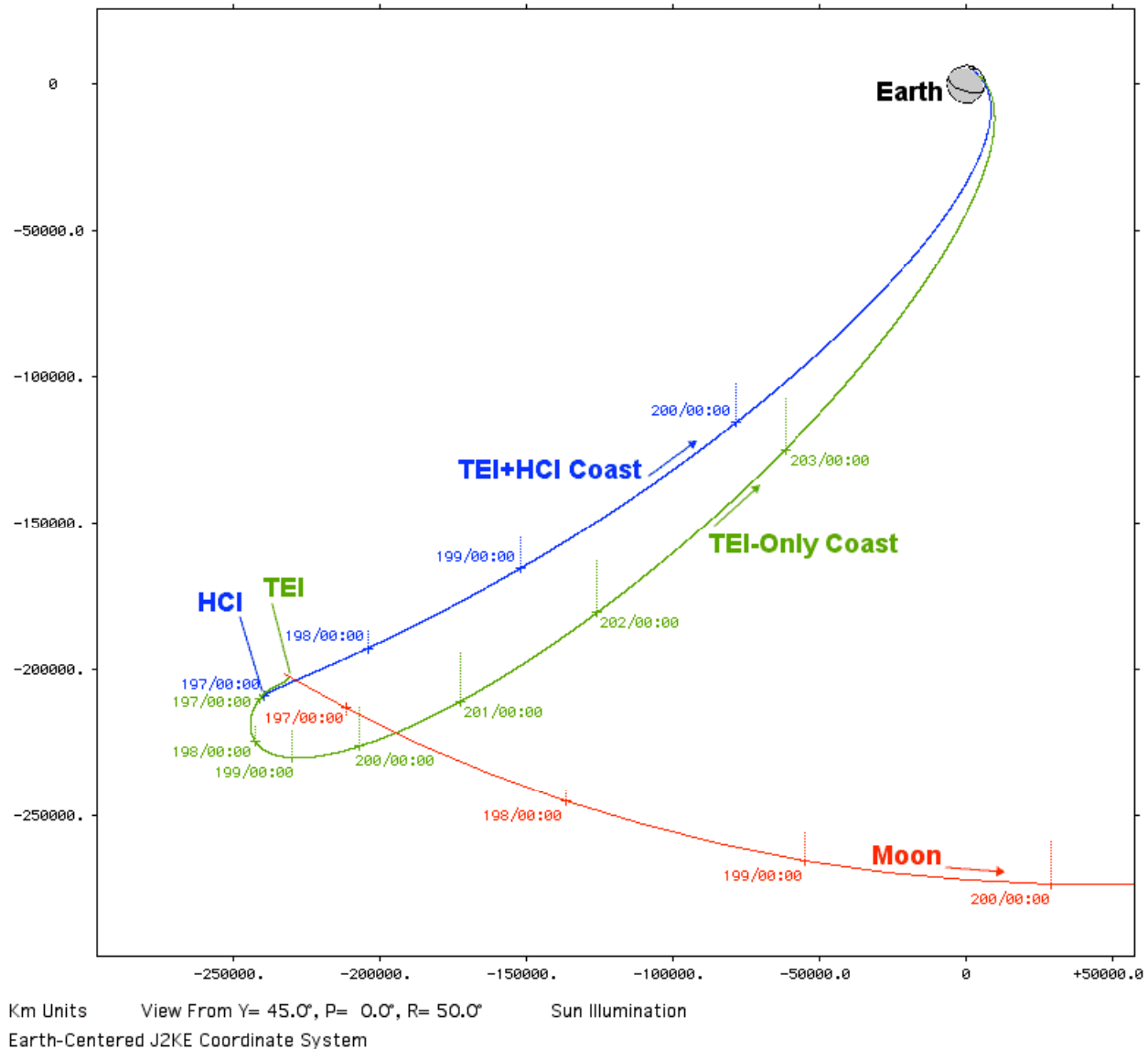


Figure 14: LLO #21 TEI+HCI Abort Trajectories

If the LLO #21 TEI+HCI abort scenario with Earth arrival on July 18 is performed entirely with DM propulsion, expended $\Delta v = 874.668 \text{ m/s}$ (nominal LOI) + 837.611 m/s (TEI) + 1243.558 m/s (HCI) = 2955.837 m/s , leaving a DM margin of $+59 \text{ m/s}$ with respect to GR&C #21. Consequently, if DM propulsion is functional throughout this scenario, no deterministic CEV impulses are required to achieve Earth arrival 4.8 days after nominal LOI. If DM propulsion is totally disabled after nominal LOI, an intact CEV has propulsive capability to perform the LLO #21 TEI impulse for Earth arrival on July 22 with $+69 \text{ m/s}$ of margin in its SM under GR&C #22, assuming prior DM jettison. This scenario results in Earth arrival 8.8 days after nominal LOI (Figure 14's green trajectory) without any HCI. If the DM only has TEI propulsive capability after a nominal LOI and is jettisoned before HCI, an intact CEV would possess a margin of -337 m/s in its SM with respect to performing the HCI achieving July 18 Earth arrival.

To address the SM capability shortfall with respect to a July 18 Earth arrival HCI, a viable alternative with respect to GR&C #22 is provided when arrival is postponed to July 19. The one-day Earth arrival delay reduces HCI Δv by 43% to 709.585 m/s . Assuming DM performs LLO #21 TEI and is jettisoned before HCI, SM margin

with respect to the reduced HCI impulse is +197 m/s. This TEI+HCI option achieves Earth arrival 5.8 days after nominal LOI (Figure 14's blue trajectory).

F. TEI+HCI Abort Summary

Practical CEV/DM aborts have been assessed following nominal LOI during LLO #1, #9, and #21, an interval spanning 39.2 hours and encompassing both viable Aristarchus Plateau landing opportunities. In accord with GR&C #21 and #22 Δv capabilities, either DM or SM propulsion can initiate Earth return by performing TEI in each of these abort scenarios. The only questionable propulsive capability associated with these scenarios lies with the degree to which HCI can speed Earth return following TEI.

The nearly polar LLO established by nominal CEV/DM LOI, in which descending nodes fall on the Moon's nearside western hemisphere, exhibits the following noteworthy TEI+HCI abort trends with progressively delayed TEI epoch. These trends are consistent with findings documented by [11].

- 1) As TEI is delayed, its Δv decreases: LLO #1 TEI $\Delta v = 902.703$ m/s, LLO #9 TEI $\Delta v = 864.801$ m/s, and LLO #21 TEI $\Delta v = 837.611$ m/s. This trend can be expected to reverse if TEI is delayed after LLO #40 or so (equivalent to July 17 at approximately 198/06:00 UTC), when lunar rotation shifts LLO descending node selenocentric λ west of -90° to the Moon's farside^{***}. Earth return initiated near the LLO #40 selenocentric plane leads to a lunar departure asymptote velocity nearly opposing the Moon's geocentric velocity, thus minimizing TEI Δv .
- 2) As TEI is delayed, coasted EI epochs in the absence of HCI become earlier. To further elaborate, the interval required to coast from TEI to EI reduces to a degree greater than the TEI delay^{†††}. This trend is illustrated in Figure 15, where the hypothetical "Break-Even" line would arise if all post-TEI coasts achieved EI on July 25 at 206/17:59:38 UTC (as is the case for a State #21 LLO #1 post-TEI coast), regardless of TEI delay. In reality, LLO #9 and #21 post-TEI coasts lead to earlier EI epochs plotted nearly 1.5 days below Figure 15's Break-Even line. Although limited CEV/DM Δv capability will eventually render TEI impractical after about July 19, EI epochs in the absence of HCI can be expected to start shifting later only when lunar rotation brings descending node selenocentric λ westward to the vicinity of 180° . Consequently, if a significant HCI is not possible and the abort does not involve serious loss of Δv capability with increasing TEI delay, Earth return can actually be expedited by remaining in LLO for the longest practical interval. It is important to note this strategy is dependent on LLO inclination and ascending node λ . It may be inappropriate for other LLO planar orientations.
- 3) As TEI is delayed, HCI Δv maintaining a specified T_E increases. For LLO #1 abort, HCI $\Delta v = 883.043$ m/s is required to achieve Earth return on July 18. For LLO #9 abort, HCI $\Delta v = 936.704$ m/s is required to achieve Earth return on July 18. For LLO #21 abort, HCI $\Delta v = 1243.558$ m/s is required to achieve Earth return on July 18. An exception to this trend is difficult to imagine because it reflects covering a nearly fixed trans-Earth distance in a progressively diminishing time interval.

^{***} With a lunar equator LLO node at a western hemisphere nearside selenocentric λ , as is the case with the three TEI+HCI abort scenarios assessed, TEI occurs over the Moon's nearside. The LLO #1 TEI is at selenocentric $\delta = -49.421^\circ$; $\lambda = -63.211^\circ$, LLO #9 TEI is at selenocentric $\delta = -44.099^\circ$; $\lambda = -69.099^\circ$, and LLO #21 TEI is at selenocentric $\delta = -40.184^\circ$; $\lambda = -80.322^\circ$. To partially oppose lunar geocentric motion and efficiently obtain low perigee after lunar escape post-TEI, a geocentric retrograde asymptotic velocity component is essential. In order to obtain this asymptotic velocity component near the assessed LLO planes, a geocentric outward component is also necessary post-TEI. It is this outward asymptotic velocity component that drives TEI location to the lunar nearside, assuming a large and inefficient selenocentric radial Δv component is to be avoided.

^{†††} Dynamics driving this trend are evident by comparing the "TEI-Only Coast" (green) trajectory plots in Figure 12, Figure 13, and Figure 14. Note the decrease in post-TEI apogee as TEI is delayed. Figure 12's post-LLO #1 TEI apogee $H = +497853$ km, Figure 13's post-LLO #9 TEI apogee $H = +448084$ km, and Figure 14's post-LLO #21 TEI apogee $H = +413473$ km. With sufficient TEI delay, trans-Earth coast will not involve any apogee passage.

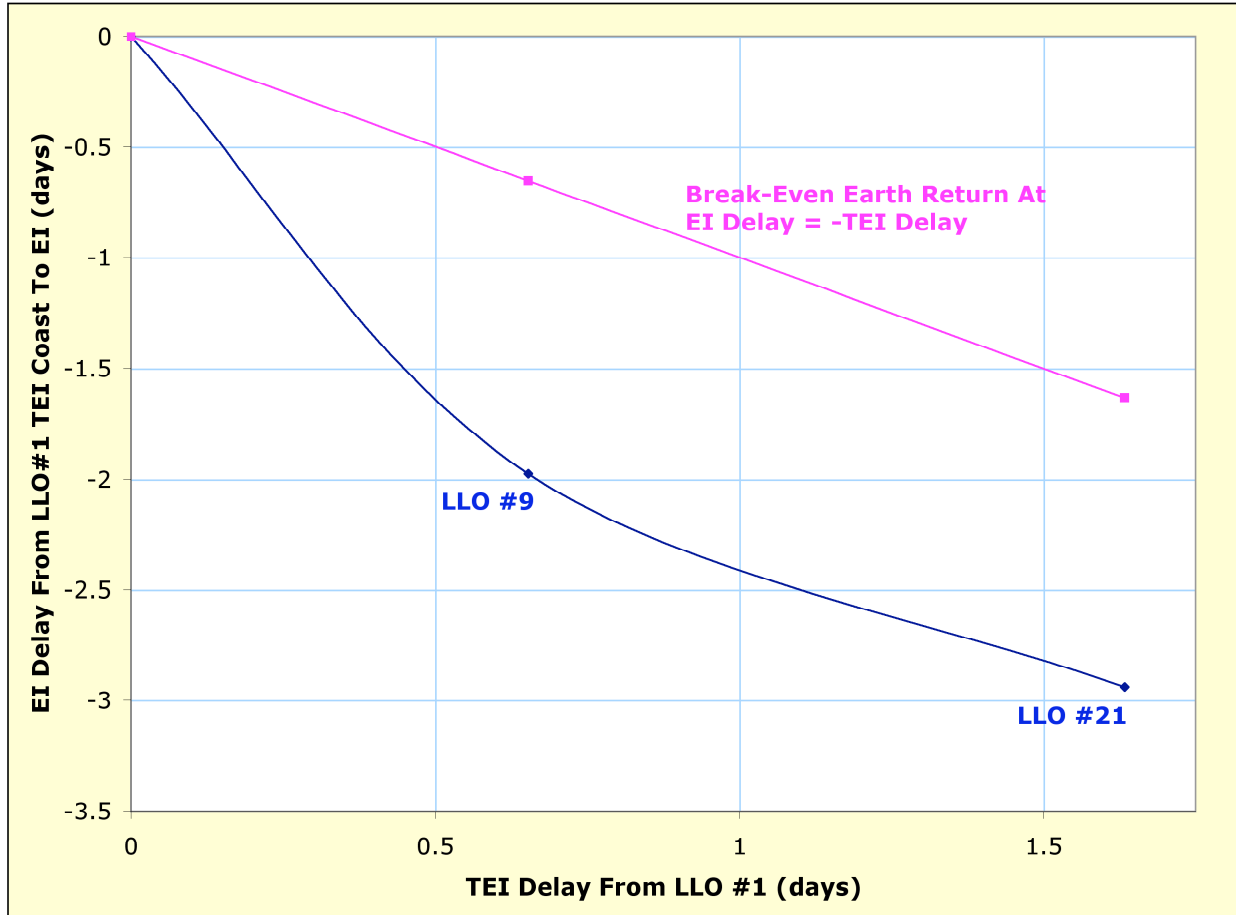


Figure 15: Delay In No-HCI Coast To EI As A Function Of TEI Delay From LLO #1

X. CEV/DM No-LOI Abort

The HCI portion of TEI+HCI abort targeting is applicable to another contingency scenario in which LOI is terminated with little or no Δv applied. This section assesses the no-LOI case, obtaining an HCI position by coasting post-TLI State #5 about 6 hours beyond the nominal LOI epoch to July 14 at 195/06:00 UTC. The requisite CSM T_E/δ iteration initiating HCI targeting from this departure point with geocentric $\delta = -16.720^\circ$ notionally restricts T_E to July 18. The associated CSM solution has T_E on July 18 at 199/18:06 UTC with geocentric arrival parameters $\delta = +10.8^\circ$, $\psi = 62.208^\circ$, $\gamma = -5.858^\circ$, and $i = 29.660^\circ$. With this CSM solution serving as initial seed to SPSM, the State #29 HCI solution results. Note HCI Δv is directed nearly 89° from the geocenter, in marked contrast to HCI solutions associated with TEI+HCI aborts from LLO^{***}.

^{***} As documented in Subsection C, Subsection D, and Subsection E, HCI Δv associated with TEI+HCI aborts from LLO is consistently directed within 2° of the geocenter. Both the large magnitude and geocentrically non-radial character of this HCI Δv are attributable to the no-LOI trajectory. Unlike a post-TEI trajectory in a TEI+HCI abort, the no-LOI trajectory will not intercept Earth and a large plane change is required to achieve this condition, regardless of the targeted T_E epoch.

State #29: CEV/DM no-LOI abort post-HCI on 2019 July 14 at 195/06:00 UTC (HCI $\Delta v = 1504.476$ m/s; coasted EI geocentric speed = 10.986 km/s on July 18 at 199/18:05:43 UTC)

$$\mathbf{r} = \begin{bmatrix} -3144.140 \\ -5673.954 \\ +26872.650 \end{bmatrix} \text{ selenocentric J2K km} \quad \mathbf{v} = \begin{bmatrix} -0.936356 \\ +0.268840 \\ +0.280480 \end{bmatrix} \text{ selenocentric J2K km/s}$$

$$i = 80.428^\circ \quad u = 98.734^\circ \quad \psi = 132.004^\circ \quad \gamma = +18.637^\circ$$

A course deviation near 90° associated with the State #29 abort is evident from Figure 16, in which State #29 (green) and #5 (blue) selenocentric coasts are co-plotted. Time ticks in this plot are annotated with UTC DOY = 194 to 195 = July 13 to 14. Dotted lines emanating from time ticks are projections onto the lunar equator plane. Shaded points of the Moon's surface are located on its farside from Earth. The Figure 16 plot is viewed from a perspective very nearly normal to the State #5 trajectory coast and identical to the Figure 10 perspective.

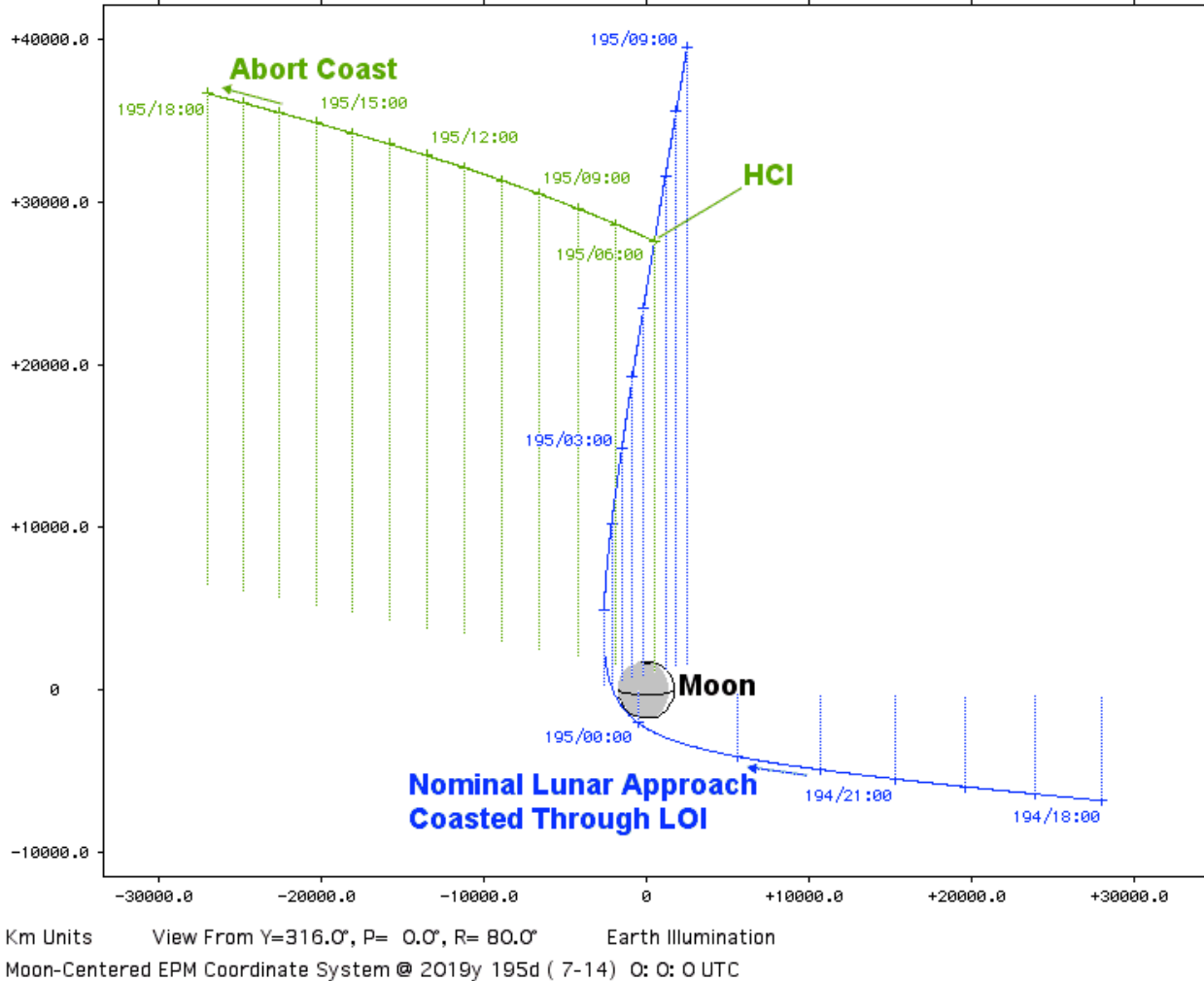


Figure 16: No-LOI HCI Abort

Note the nearly parallel incoming pre-pericyynthion and outgoing post-HCI asymptotic velocities from Figure 16. In effect, HCI Δv must undo the gravity assist imparted by the Moon to the no-LOI CEV/DM trajectory. Although considerably more propellant-intensive than a circumlunar abort performed pre-LOI, the no-LOI HCI Δv is well within nominal DM propulsive capability. Since the DM expends no propellant on LOI in this scenario, a DM margin of +1511 m/s with respect to GR&C #21 is obtained. On the other hand, no-LOI HCI Δv exceeds SM propulsive capability. With respect to GR&C #22, the SM margin for this impulse is -597 m/s.

XI. CEV/DM No-LOI Rescue

Consider a CEV/DM with no propulsive capability post-TLI. Even if TLI targeted a circumlunar free-return trajectory, this scenario would most likely produce a trajectory missing the Moon and Earth. The cumulative effect of unanticipated perturbations left uncorrected by propulsion during cislunar "coast" would therefore necessitate a rescue, even under conservative free-return TLI targeting. This rescue will be flown by a functional CEV/DM, either remotely piloted or launched with a minimal crew, and complying with every pertinent GR&C outlined in Section IV. In the following narrative, the vehicle without onboard propulsion is called the "disabled CEV"^{§§§}, and the functional vehicle is called the "rescue CEV/DM".

To illustrate rescue CEV/DM capability in a variety of demanding scenarios, the disabled CEV is assumed to be on the coasted post-TLI trajectory defined by State #5. After coasting through LOI and departing the Moon (reference Figure 16's blue selenocentric trajectory plot), the disabled CEV is likely on its way to solar orbit. Perigee occurs on July 14 at 195/22:44:46 UTC (22.6 hours after pericyynthion and nominal LOI) with geocentric $H = 377167$ km and $i = 42.053^\circ$.

Rescue CEV/DM mission design begins with POM and SPSM targeting of an Earth parking orbit supporting 3-day transit from LEO departure at trans-rescue injection (TRI) to disabled CEV intercept, assuming launch on July 15. This parking orbit satisfies geometry imposed by GR&C #2, #3, and #6. When GR&C #4 accelerations are modeled, the SPSM parking orbit solution is expressed as the following state vector.

State #30: rescue CEV/DM instantaneous KSC launch on 2019 July 15 at 196/08:38 UTC

$$\mathbf{r} = \begin{bmatrix} +5477.683 \\ -1823.904 \\ +3121.396 \end{bmatrix} \text{ geocentric J2K km} \qquad \mathbf{v} = \begin{bmatrix} +2.441079 \\ +7.403721 \\ +0.042726 \end{bmatrix} \text{ geocentric J2K km/s}$$

$$i = 28.502^\circ \qquad u = 89.275^\circ \qquad \psi = 89.606^\circ \qquad \gamma = +0.001^\circ$$

Because Earth gravity is predominant throughout the post-TRI coast to disabled CEV intercept, CSM targeting of this arc is highly accurate. Fixing intercept on July 18 at 199/11:00 UTC, a close geocentric ψ match with the coasted State #30 trajectory is achieved for TRI on July 15 at 196/10:47 UTC. When this CSM solution seeds SPSM, it is only necessary to shift intercept to July 18 at 199/10:00 UTC in order to maintain the TRI ψ match, and State #31 results.

State #31: rescue CEV/DM post-TRI on 2019 July 15 at 196/10:47 UTC (TRI $\Delta v = 3213.039$ m/s)

$$\mathbf{r} = \begin{bmatrix} -4860.048 \\ +3196.597 \\ -3038.814 \end{bmatrix} \text{ geocentric J2K km} \qquad \mathbf{v} = \begin{bmatrix} -5.561530 \\ -9.412757 \\ -1.277837 \end{bmatrix} \text{ geocentric J2K km/s}$$

$$i = 28.533^\circ \qquad u = 256.473^\circ \qquad \psi = 97.248^\circ \qquad \gamma = +0.653^\circ$$

Shortly before intercept, the rescue CEV/DM must generate $\Delta v = 1201.496$ m/s to null its closing rate with the disabled CEV. This rendezvous and subsequent proximity operations between two vehicles at geocentric $H = 457000$ km and beyond will be unlike any conducted at low Earth or Moon orbit heights. A perceivable gravity gradient between the rescue CEV/DM and disabled CEV will be absent over distances of many km, greatly simplifying any piloting tasks.

Rescue CEV/DM Earth return is notionally initiated on July 19 at 200/10:00 UTC, one day after disabled CEV intercept. The disabled CEV geocentric position at that epoch ($H = 499090$ km and $\delta = +30.618^\circ$), as coasted from State #5, serves as the CSM departure boundary condition for T_E/δ iteration with T_E notionally restricted to July 22. This iteration is subject to GR&C #19 and #20 Earth return geometry. The resulting CSM solution has T_E on July 22 at 203/21:02 UTC with geocentric arrival parameters $\delta = -34.0^\circ$, $\psi = 88.885^\circ$, $\gamma = -5.809^\circ$, and $i = 34.016^\circ$. With this CSM solution serving as initial seed to SPSM, the State #32 TEI solution results.

^{§§§} Whether or not the disabled CEV has jettisoned its DM is assumed insignificant to this rescue's feasibility. Depending on circumstances relating to abandoning the nominal mission, DM jettison may or may not be advisable.

State #32: rescue CEV/DM post-TEI on 2019 July 19 at 200/10:00 UTC (TEI $\Delta v = 1823.089$ m/s; coasted EI geocentric speed = 11.062 km/s on July 22 at 203/21:01:58 UTC)

$$\mathbf{r} = \begin{bmatrix} +344727.795 \\ -265932.144 \\ +256788.619 \end{bmatrix} \text{ geocentric J2K km} \quad \mathbf{v} = \begin{bmatrix} -0.630412 \\ +0.657699 \\ -0.566942 \end{bmatrix} \text{ geocentric J2K km/s}$$

$i = 32.896^\circ$ $u = 110.321^\circ$ $\psi = 102.660^\circ$ $\gamma = -82.551^\circ$

An overview of the entire rescue scenario is illustrated by Figure 17, in which State #5 (green) and #31/#32 (blue) geocentric coasts are co-plotted. Time ticks in this plot are annotated with UTC DOY = 192 to 203 = July 11 to 22. Dotted lines emanating from time ticks are projections onto the ecliptic plane. Shaded points of Earth's surface are in darkness.

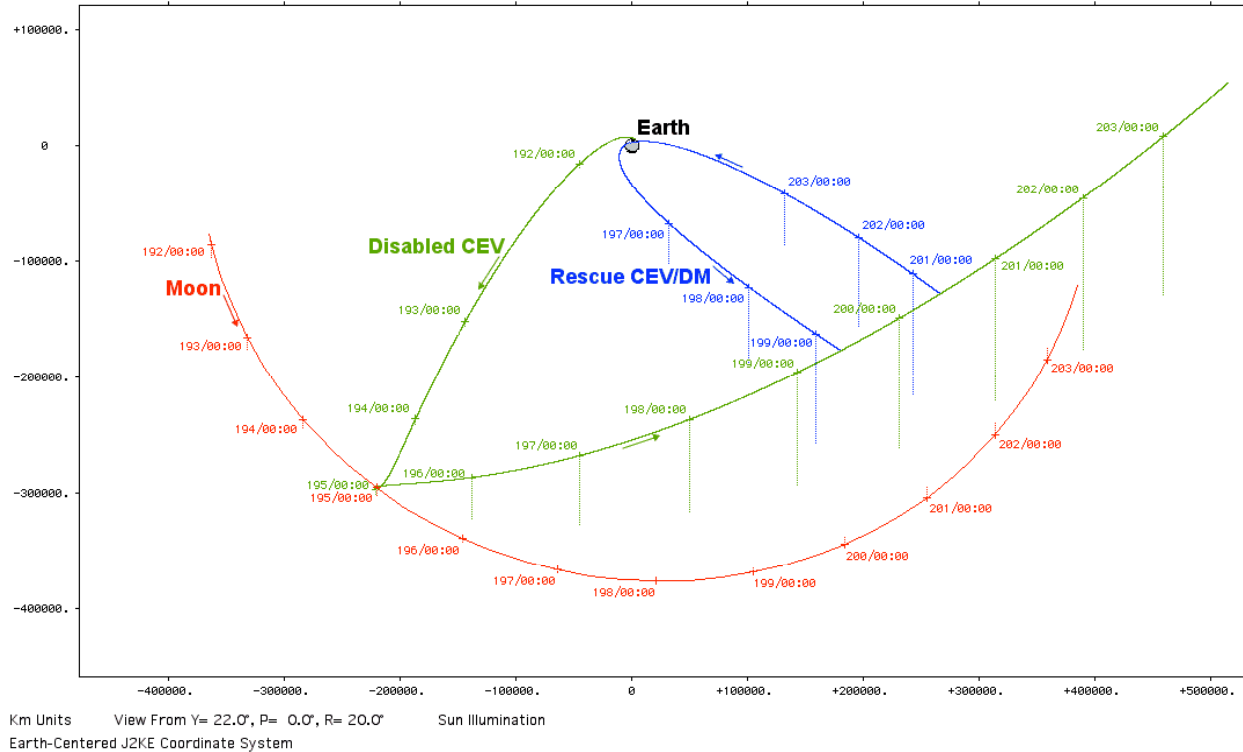


Figure 17: A Disabled CEV Rescue Mission

Rescue CEV/DM impulses required at disabled CEV intercept and TEI equate to a total $\Delta v = 1201.496 + 1823.089 = 3024.585$ m/s. With respect to GR&C #21 DM capability, this total is excessive with a margin of -10 m/s. Assuming the rescue scenario is not urgent, even small increases to rescue CEV/DM outbound and return transit time intervals could yield a positive DM Δv margin. Given an additional $\Delta v = 907$ m/s SM capability under GR&C #22, this may not be necessary. However, it should be noted TRI $\Delta v = 3213.039$ m/s is some 60 m/s greater than nominal TLI impulses supporting this LSR mission design. As an alternative to longer outbound transit time, offloading the rescue CEV/DM of sufficient CM human consumables and SM propellant mass can provide additional TRI capability as required.

To provide the rapid response necessary in this rescue scenario, adequate launch pad logistics are critical. If both Pad A and Pad B at KSC's LC-39 are presumed to be Ares V-capable with either RCM/DM or CEV/DM payloads, these logistics may be realizable. In this rescue scenario, a plausible logistics example would entail RCM/DM launch on June 11 from Pad A, disabled CEV launch on July 10 from Pad B, and rescue CEV/DM launch on July 15 from Pad A. Preparations for the rescue CEV/DM launch from Pad A would begin soon after the RCM/DM launch. In the likely event a rescue is not required, the rescue CEV/DM and its Ares V would be used in the next lunar mission. The *Skylab* Program employed a similar rescue vehicle logistics strategy [12].

As it escapes from a perigee near the Moon's orbit to an Earth-similar solar orbit, this scenario's disabled CEV trajectory plausibly exemplifies one of the most accessible near-Earth object (NEO) trajectories imaginable. The rescue CEV/DM trajectory developed here may therefore be regarded as a nearly minimal-distance NEO roundtrip

completed in nearly minimal time. Consequently, this viable rescue assessment also serves to demonstrate Ares V/CEV/DM performance capable of NEO exploration to at least a minimal degree.

XII. Conclusion

Table 5 summarizes major events associated with the nominal Aristarchus Plateau mission design documented by this paper. Each maneuver Δv in Table 5 is accompanied by a steering loss (SL) value indicating the degree to which each impulse is purely posigrade or retrograde with respect to the pertinent trajectory plane and reference body. An SL value is computed by subtracting magnitude of the posigrade/retrograde impulse component from the corresponding Δv . Under this convention, SL quantifies propulsive expenditures in addition to unavoidable kinetic energy changes required to initiate or terminate trans-lunar or trans-Earth flight. These efficiency losses are associated with imparting a plane change and/or a modified rate of climb/descent. During the RCS/DM mission, SL totals 3.362 m/s, and SL's sum during the nominal CEV/DM mission is 0.346 m/s.

These negligible SL values indicate LSR trajectory targeting techniques documented by this paper can be applied to any lunar surface destination with minimal Δv variations. Changes in Δv costs among other LSR mission designs are expected to result chiefly from lunar geocentric distance variations and the minor deviations in trans-lunar/trans-Earth transit time they and other mission design constraints impose. This is in marked contrast to lunar approach strategies seeking to maintain circumlunar Earth free return until lunar arrival and often requiring a dedicated plane change to achieve LOI. Likewise, trajectory targeting strategies documented herein and made possible by LSR architecture do not require dedicated plane change impulses to achieve LLO rendezvous or TEI supporting anytime Earth return.

Table 5: A Notional Lunar Surface Rendezvous Mission Profile To Aristarchus Plateau

2019 Date	UTC	Event
June 11	162/19:39	Ares V launches RCM/DM into LEO: $H = +185$ km, $\psi = 89.6^\circ$, $i = 28.5^\circ$.
June 11	162/22:24	EDS achieves RCM/DM TLI: $\Delta v = 3147.214$ m/s, $SL = 3.362$ m/s.
June 15	166/02:56	RCM/DM achieves lunar approach targets: $H = +1500$ km, $\delta = -60.5^\circ$, $\lambda = -90^\circ$.
June 15	166/03:21	DM achieves RCM/DM LOI: $\Delta v = 862.304$ m/s, $SL = 0$, $H = +100$ km, $i = 109.5^\circ$.
June 15	166/16:09	RCM/DM LLO #7 landing at Aristarchus Plateau: local solar elev = $+13.8^\circ$.
July 10	191/18:22	Ares V launches CEV/DM into LEO: $H = +185$ km, $\psi = 89.5^\circ$, $i = 28.5^\circ$.
July 10	191/21:10	EDS achieves CEV/DM TLI: $\Delta v = 3151.525$ m/s, $SL = 0.318$ m/s.
July 13	194/23:50	CEV/DM achieves lunar approach targets: $H = +1028$ km, $\delta = -71.5^\circ$, $\lambda = -90^\circ$.
July 14	195/00:09	DM achieves CEV/DM LOI: $\Delta v = 874.668$ m/s, $SL = 0$, $H = +100$ km, $i = 102.9^\circ$.
July 14	195/14:56	CEV/DM LLO #8 landing at Aristarchus Plateau: local solar elev = $+8.6^\circ$.
July 21	202/17:04	CEV launch into LLO: $H = +100$ km, $\psi = 87.2^\circ$, $i = 26.1^\circ$, local solar elev = $+63.7^\circ$.
July 21	202/20:48	CEV achieves TEI: $\Delta v = 916.729$ m/s, $SL = 0.028$ m/s.
July 24	205/23:47	CEV entry interface: speed = 11.010 km/s, $\psi = 57.5^\circ$, $\gamma = -5.7^\circ$, $\delta = -2.9^\circ$, $\lambda = -140.0^\circ$.

In addition to nominal LSR mission design, this paper has documented multiple CEV/DM abort options resulting in Earth return to primary recovery conditions. These options indicate continuous abort coverage is available from TLI until commitment to lunar landing during powered descent. Throughout much of this time interval, redundant abort capability exists, with either of the major and independent propulsive systems aboard CEV/DM having the capacity to return the crew to Earth. This paper has also demonstrated abort and rescue options even in the event no CEV/DM propulsion is available prior to LOI and assuming lunar approach grossly deviates from a circumlunar Earth free-return trajectory.

Robust and consistent performance demonstrated in association with nominal, abort, and rescue LSR mission planning is essential to satisfying the "land anywhere; leave anytime" requirement levied by United States Space Exploration Policy. The author is prepared to further demonstrate and assess associated LSR attributes on request.

References

- [1] Adamo, D. R., "Revisited Virtues of Lunar Surface Rendezvous (LSR)", 21 January 2009.
- [2] NASA, "Exploration Systems Architecture Study Final Report", NASA-TM-2005-214062, November 2005, www.nasa.gov/directorates/esmd/news/ESAS_report.html [retrieved 7 November 2008].
- [3] Brown, C. D., *Spacecraft Mission Design*, AIAA, 1992.
- [4] Adamo, D. R., *A Uniform Solution of the Lambert Problem Derived from Sperling's Equation*, University of Houston at Clear Lake City Master's Thesis, 1981.
- [5] Adamo, D. R., "A Precision Orbit Predictor Optimized For Complex Trajectory Operations," *Astrodynamics 2003, Advances in the Astronautical Sciences*, Vol. 116, Univelt, San Diego, CA, 2003, pp. 2567-2586.
- [6] Adamo, D. R., "Apollo 13 Trajectory Reconstruction via State Transition Matrices", *Journal of Guidance, Control, and Dynamics*, Vol. 31, No. 6, 2008, pp. 1772-1781.
- [7] *Lunar Capability Concept Review (LCCR)*, Constellation Program, 18 - 20 June 2008, www.lpi.usra.edu/pss/presentations/200806/12neal.pdf [accessed 21 January 2009].
- [8] Giorgini, J. D., Yeomans, D. K., Chamberlin, A. B., Chodas, P. W., Jacobson, R. A., Keesey, M. S., Lieske, J. H., Ostro, S. J., Standish, E. M., Wimberly, R. N., "JPL's On-Line Solar System Data Service", *Bulletin of the American Astronomical Society*, Vol. 28, No. 3, 1996, p. 1158.
- [9] *Aristarchus LAC 39*, USAF Aeronautical Chart And Information Center, November 1963, www.lpi.usra.edu/resources/mapcatalog/LAC/lac39/ [retrieved 6 January 2009].
- [10] Orloff, R. W. and Harland, D. M., *Apollo: The Definitive Sourcebook*, Springer-Praxis, 2006.
- [11] Adamo, D. R., "A 2-Stage Earth Return Targeting Strategy From Polar Low Lunar Orbit", 23 July 2008.
- [12] "Skylab Rescue", http://en.wikipedia.org/wiki/Skylab_Rescue [retrieved 20 February 2009].